Anti-platelet properties of Pim kinase inhibition is mediated through disruption of thromboxane A2 receptor signalling.

Amanda J. Unsworth*[1,2], Alexander P. Bye[1], Tanya Sage[1], Renato S Gaspar[1], Nathan Eaton[3,4], Caleb Drew[3], Alexander Stainer[1], Neline Kriek[1], Peter J. Volberding[3,4,5], James L. Hutchinson[6], Ryan Riley[2], Sarah Jones[2], Stuart J. Mundell[6], Weiguo Cui[3,4,5], Hervé Falet[3,4], Jonathan M. Gibbins*[1]

* Authors contributed equally.

[1] Institute for Cardiovascular and Metabolic Research, School of Biological Sciences, Harborne building, University of Reading, Whiteknights, Reading, RG6 6AS, UK

[2] Department of Life Sciences, Faculty of Science and Engineering , John Dalton Building, Manchester Metropolitan University, Manchester, UK, M1 5GD

[3] Blood Research Institute, Versiti, Milwaukee, WI 53226, USA

[4] Department of Cell Biology, Neurobiology, and Anatomy, Medical College of Wisconsin, Milwaukee, WI 53226, USA

[5] Department of Microbiology and Immunology, Medical College of Wisconsin. Milwaukee, WI 53226, USA

[6] School of Physiology, Pharmacology & Neuroscience, Biomedical Sciences Building, University Walk, Bristol BS8 1TD

Corresponding author: A.J. Unsworth, Department of Life Sciences, Faculty of Science and Engineering, John Dalton Building, Manchester Metropolitan University, Manchester, UK, M1 5GD, telephone: +441612472945, email: a.unsworth@mmu.ac.uk

Short title: Pim kinase regulates TP receptor signalling

Conflict of interest statement

The authors have declared that no conflict of interest exists.

ABSTRACT

Pim kinases are upregulated in several forms of cancer, contributing to cell survival and tumour development, but their role in platelet function and thrombotic disease has not been explored.

We report for the first time that Pim-1 kinase is expressed in human and mouse platelets. Genetic deletion or pharmacological inhibition of Pim kinase results in reduced thrombus formation but is not associated with impaired haemostasis. Attenuation of thrombus formation was found to be due to inhibition of the thromboxane A2 receptor as effects on platelet function was non-additive to inhibition caused by the cyclooxygenase inhibitor indomethacin or thromboxane A2 receptor antagonist GR32191. Treatment with Pim kinase inhibitors caused reduced surface expression of the thromboxane A2 receptor and resulted in reduced responses to thromboxane A2 receptor agonists, indicating a role for Pim kinase in the regulation of thromboxane A2 receptor function.

Our research identifies a novel, Pim kinase dependent regulatory mechanism for the thromboxane A2 receptor and represents a new targeting strategy that is independent of COX-1 inhibition or direct antagonism of the thromboxane A2 receptor that whilst attenuating thrombosis does not increase bleeding.

INTRODUCTION

The family of Pim (proviral insertion in murine lymphoma) kinases, Pim-1, -2, and -3 are highly homologous serine/threonine kinases that are widely expressed across several cell types, and are expressed highly in haematopoietic cells. Pim kinases are constitutively active and are linked with cancer progression [1,2], with over-expression and upregulation of Pim kinase activity associated with both haematological and solid tumour cancers. They function by phosphorylating their target proteins on serine/threonine residues located within the common consensus sequence ARKRRHPS*GPPTA [1]. A number of proteins that have important roles in the regulation of cellular proliferation and survival have been identified as phosphorylation targets of the Pim kinases [3-6]. Expressed as a short (32 kDa) or long (44 kDa) variant, the longer variant of Pim-1 kinase, Pim-1L, kinase has also been found to regulate adenosine triphosphate-binding cassette (ABC) drug transporters [7-9]. Pim-1 phosphorylates both BCRP/ABCG2 and Pgp transporters enabling, through different mechanisms, the formation of drug efflux pumps [7,9].

Pim kinases are highly expressed in hematopoietic cells where they are important for differentiation and development of blood cells and blood cell precursors including megakaryocytes [10] and platelets [11]. Whether Pim kinases are involved in the regulation of platelet function has not been explored. Analysis of the mouse megakaryocyte transcriptome database [12] identified multiple tags for both Pim-1 and Pim-2 kinases and the mRNA transcripts for all three Pim kinases have been identified in the human platelet transcriptome [13,14]. Interestingly although triple knock-out mice deficient in all three Pim kinase isoforms are viable, they have been shown to have altered haematopoiesis, but there is some dispute as to whether disruption of all three isoforms results in alteration of platelet count [10,11], however, platelet counts appear to be unaffected by alteration of Pim-1 expression levels in mice [15,16].

Platelets rely on G protein coupled receptors (GPCRs) such as the Thromboxane A2 receptor (TPαR), ADP receptors (P2Y1 and P2Y12) and the thrombin receptors (PAR1 and PAR4) to mediate platelet activation in response to vessel damage. All platelet GPCRs are regulated in

some way by receptor cycling/internalisation from the platelet surface as well as desensitisation [17]. Pim-1 kinase has also been shown to have a role in the regulation of G protein coupled receptor (GPCR) function, through modulation of surface levels of the CXCR4 receptor [18,19]. Inhibition of Pim kinase prevents Pim kinase dependent phosphorylation of CXCR4 at Ser339 and modification of the CXCR4 intracellular C terminal domain resulting in reduced surface expression and signalling. In this study we report the presence of Pim-1 in human and mouse platelets, and reduced thrombosis in Pim-1 null mice, and following pharmacological inhibition of Pim kinase, but with no associated effect on haemostasis. We describe a novel mechanism of action by which Pim kinase inhibitors negatively regulate thromboxane A2 receptor (TPαR) signalling.

METHODS

Procedures and experiments using human blood were approved by the University of Reading Research Ethics Committee and protocols using mice were performed according to the National Institutes of Health and Medical College of Wisconsin Institutional Animal Care and Use Committee guidelines and as following procedures approved by the University of Reading Research Ethics Committee.

Platelet isolation, thrombus formation assays, tail bleeding experiments, platelet function tests, aggregometry, granule secretion, flow cytometry, calcium imaging, immunoblotting, image analysis, statistical analyses and materials used are described in Supplemental Methods.

RESULTS

Expression of Pim kinase in human and mouse platelets

Pim kinases are highly expressed in hematopoietic cells [10,11]. mRNA transcripts for all three Pim kinases have been identified in the human and mouse platelet transcriptomes [13,14] and

HaemAtlas mRNA expression profiles in haematopoetic cells [20] show high expression of Pim-1 in megakaryocytes and moderate expression in platelets (Figure 1 and Supplemental Figure 1) [21].Western blot analysis of platelet lysates identified a protein band of 44kDa apparent molecular mass in both human and mouse platelet lysates indicating the expression of the larger Pim-1 variant (Pim-1L). A protein band at 32 kDa in mouse platelets also suggested expression of the smaller Pim-1S. K562 and Jurkat cell lines were included as positive controls [8,18,22] (Figure 1B).

Reduced thrombus formation in Pim-1 deficient mice

To determine whether Pim-1 plays a role in the regulation of platelet function and thrombosis, we measured the ability of Pim-1 deficient mouse platelets taken from constitutive Pim-1 deficient mice to form thrombi on collagen under arterial flow *in vitro*. Constitutive *Pim1*$^{-/-}$ mice were as described previously [15,16] and global deletion of Pim-1 confirmed by PCR analysis of genomic DNA (supplemental figure 2A). Mouse whole blood from Pim-1$^{-/-}$ or Pim-1$^{+/-}$ mice was perfused over collagen-coated (100 µg/mL) Vena8 biochips for 4 minutes at an arterial shear rate of 1000 s^{-1}. Thrombus formation was significantly attenuated in blood from Pim-1$^{-/-}$ mice compared to controls, indicating Pim-1 plays a positive role in the regulation of platelet function and thrombus formation on collagen (Figure 2A). Constitutive Pim-1$^{-/-}$ mice show unaltered platelet counts and no difference in expression levels of major platelet adhesion receptors GPIbα, GPIbβ, GPIX, GPV, GPVI and integrins β1 and β3 was observed in Pim-1$^{-/-}$ platelets compared to controls (supplemental figure 2B). Interestingly, despite the reduced ability to form thrombi, Pim-1 deficient mice showed no alteration in haemostasis as tail bleeding was unaffected compared to littermate controls (Figure 2B).

Pim kinase inhibitors reduce thrombus formation but do not disrupt haemostasis.

As genetic deletion of Pim-1 in mice resulted in reduced *in vitro* thrombus formation, we assessed the effects of the Pim kinase inhibitor AZD1208 (100 µM) on thrombus formation in human whole blood. The effect of the Pim kinase inhibitor AZD1208 (100 µM) on thrombus

formation on collagen in human whole blood *in vitro* was also assessed. Human whole blood was pre-incubated with vehicle control or AZD1208 and perfused over collagen-coated (100 µg/mL) Vena8 biochips at either an arterial shear rate (20 dynes/cm^3 for 10 mins) or pathological shear rate (135 dynes/cm^3 for 5 mins). Similar to that observed in Pim-1 deficient mice, a reduction in thrombus formation and stability on collagen under flow *in vitro* was also observed following AZD1208 treatment in comparison to vehicle treated controls under arterial shear conditions (figure 2C). Whilst thrombus size and stability appeared reduced at arterial flow rates, the early stages of thrombus formation, including initial adhesion, appeared unaffected by AZD1208 treatment. This is further supported by lack of inhibition of platelet adhesion and spreading on collagen by AZD1208 under static conditions (supplemental figure 3), indicating that the initial adhesion to collagen is not affected by Pim kinase inhibition. Interestingly, enhanced inhibition of thrombus formation on collagen was observed following treatment with AZD1208 at pathological shear rates (~80% inhibition) Figure 2D) in comparison to the inhibition observed at arterial shear (~50% inhibition). In contrast to arterial and pathological shear rates, a slight (but not significant) reduction in thrombus formation was observed in AZD1208 treated platelets compared to vehicle treated controls under venous shear conditions (Figure 2E). Inhibitor treated platelets appeared to form 'woolly' or 'loose' aggregates compared to vehicle controls, but no difference in fluorescence intensity of platelets adhered was observed. These findings indicate Pim kinase inhibition does not significantly alter platelet adhesion and thrombus formation at low shear rates compared to the effects observed at higher shear rates. To examine whether Pim kinase inhibition could regulate thrombosis in vivo, we performed intravital microscopy following ferric-chloride-induced injury in mice pretreated with AZD1208 (100 µM) or vehicle control (Figure 2F). As with in vitro thrombus formation, treatment with AZD1208 resulted in a dramatic attenuation in the ability of platelets to form thrombi in vivo at the site of FeCl3 injury with significantly prolonged occlusion times observed in AZD1208 treated mice (1463 ± 37 secs) compared to vehicle treated controls (697 ± 72 secs). This supports a role for Pim kinase in the positive regulation of platelet function, and the anti-platelet properties of Pim kinase inhibitors.

Interestingly, despite the dramatic attenuation in the ability of platelets to form thrombi in vivo, as with genetic deletion, pharmacological inhibition of Pim kinase was not associated with altered haemostasis. Tail bleeding assays performed in mice indicated that treatment with AZD1208 (100 µM) did not cause any significant increase in bleeding (Figure 2G), suggesting that despite the observed inhibitory effect on thrombus formation, normal haemostasis is not compromised following inhibition or genetic deletion of Pim kinase.

Pim kinase inhibitors reduce platelet aggregation

To determine how Pim kinase plays a role in the regulation of platelet function, human washed platelets were pretreated for 10 minutes with a range of concentrations of the pan-Pim kinase inhibitor AZD1208 before stimulation with platelet agonists. As shown in Figure 3A-E pre-treatment of platelets with AZD1208 inhibited aggregation stimulated by collagen (1 µg/mL) or the thromboxane A_2 (TxA_2) mimetic U46619 (0.3 µM). A slight inhibition was also observed in CRP-XL stimulated platelets (0.3 µg/mL). In contrast no inhibition of thrombin (0.03 U/mL) or ADP (10 µM) induced platelet aggregation was observed following treatment with increasing concentrations of AZD1208 (up to 10 µM). Treatment with four other structurally unrelated Pim kinase inhibitors PIM-447 (LGH-447), SGI-1776, SMI-4a and CX6258 inhibited platelet aggregation stimulated by both collagen or U46619 but not thrombin, recapitulating findings with AZD1208 and supporting a Pim kinase-dependent mode of action (Supplemental figure 4).

Pim kinases have been shown previously to play important roles in cell survival as Pim-2 is known to phosphorylate and inactivate Bcl-2-associated death promoter (BAD) [23]. Inhibition of Pim kinase enables activation of BAD and initiation of apoptosis [5]. If Pim kinase inhibitors activate apoptosis in platelets, this could cause the observed reduction in aggregation. To investigate whether Pim kinase inhibition triggers apoptosis in platelets, phosphatidylserine exposure (a marker of membrane flippage) was determined by measuring Annexin V binding by flow cytometry following treatment for 2 hr with AZD1208 or BCL-2 inhibitor ABT-263, an activator of apoptosis in platelets (Supplemental Fig 5A). ABT-263 treatment caused an

increase in Annexin V binding but no difference was observed in AZD1208 treated platelets compared to vehicle treated controls over following the same incubation time. Furthermore, caspase cleavage did not occur in platelets following 2 hr treatment with Pim kinase inhibitors: AZD1208 (10μM), SGI-1776 (10μM), SMI-4a (30μM) or CX6258 (10μM), but did occur following treatment with the BCL-2 inhibitor ABT-263 (Supplemental Figure 5B). Together these observations suggest that Pim kinase inhibition does not initiate platelet apoptosis.

Pim kinase inhibitors reduce TxA_2 mediated α-granule secretion and integrin activation

Alpha granule secretion and activation of integrin $\alpha_{IIb}\beta_3$ are critical events in platelet activation that underpin platelet activation and aggregation. We investigated the effects of AZD1208 (10 μM) on alpha granule secretion and $\alpha_{IIb}\beta_3$ activation by measuring surface P-selectin exposure and fibrinogen binding respectively. AZD1208 (10 μM) inhibited alpha granule secretion and integrin activation evoked by collagen, CRP-XL and U46619 compared to vehicle treated controls (supplemental Figure 6). This suggests that Pim kinase inhibitors inhibit aggregation by reducing both integrin activation and secretion of granule contents.

Pim kinase inhibitors reduce platelet activation to GPVI via reduced TPαR signalling

TxA_2 is synthesised and released following platelet activation by several platelet agonists. It acts as a secondary mediator, boosting platelet responses to other agonists, and is essential for the amplification of platelet activation and thrombus formation. Further investigation of the inhibitory actions of AZD1208, identified significant inhibition of U46619 evoked aggregation with IC_{50} values < 10μM, concentrations similar to those achieved in plasma in patients taking AZD1208 [24], following stimulation by low concentrations of U46619 (0.03-1 μM) (Figure 4A). In contrast the inhibitory activity of AZD1208 could be overcome at higher concentrations of U46619 (3, 10 μM). Collagen induced platelet activation is known to be dependent on the release of secondary mediators. To test whether the inhibition of collagen induced platelet aggregation by AZD1208 was a result of reduced activation of the TPαR, platelet aggregation to a range of collagen concentrations was measured following treatment with AZD1208 (10

μM). We performed the experiments in the presence or absence of indomethacin (10 μM), a cyclooxygenase (COX) inhibitor that prevents TxA_2 synthesis, or TPαR antagonist GR32191 (100 nM) to investigate if inhibition was additive. As shown in Figure 4B, both indomethacin and GR32191 caused an inhibition of collagen-induced platelet aggregation, but this was not additive to the inhibition caused by AZD1208, suggesting that AZD1208 shares a common TPαR.-dependent mechanism. The inhibition observed in collagen stimulated platelets is likely due to the loss of TxA_2 signalling, indicating that Pim kinase has a positive regulatory role in the regulation of TPαR signalling. Similar results were also observed following treatment with structurally unrelated Pim kinase inhibitors SGI-1776, PIM-447 (LGH447), SMI-4a and CX6258 in the presence or absence of indomethacin (Supplemental Figure 4D-G). In further support of this, we also observed that AZD1208 mediated inhibition of thrombus formation on collagen under flow occurred via a TPαR dependent mechanism, as indomethacin (10 μM) did not cause further inhibition of thrombus formation when combined with AZD1208 treatment (Figure 4C). In support of the effects of AZD1208 being mediated via Pim kinase, and a role for Pim kinase in the regulation of platelet TPαR signalling, platelets from $Pim1^{-/-}$ mice (red) displayed reduced fibrinogen binding following stimulation with U46619 (10 μM) or CRP-XL (10 μg/mL) but not following stimulation with thrombin (0.01 U/mL) compared to controls (black) (Figure 4D).

Pim kinase inhibitors inhibit platelet function independently of COX1.

The synthesis of TxA_2 in platelets is dependent on activation of COX1 following platelet stimulation. To determine whether the inhibitory effects of Pim kinase inhibitors were due to altered COX activity, TxB_2 levels (a marker of TxA_2 release) were determined following stimulation of platelets with arachidonic acid (a direct substrate for COX-1 and the TxA2 synthesis pathway) or collagen and compared to indomethacin, a COX1 inhibitor in the presence of TPαR antagonist GR32191 to remove secondary TPαR feedback mechanisms. Whilst indomethacin caused almost complete ablation of both collagen and arachidonic acid induced platelet TxB_2 generation AZD1208 did not cause any significant alterations in TxB_2

generation indicating it does not regulate COX-1 activity (Figure 5A). In further support of AZD1208 mediating its inhibitory actions via inhibition of TPαR receptor signalling and not inhibition of cyclooxygenase activity, whilst AZD1208 causes inhibition of U46619 mediated platelet aggregation, concentrations of indomethacin that cause ablation of platelet responses to arachidonic acid, are unable to inhibit platelet activation by TPαR agonist U46619 (Figure 5A).

Pim kinase inhibitors reduce signalling events downstream of TPαR

The TPαR receptor is coupled to both G_q and $G_{\alpha 13}$ proteins. G_q couples the TPαR to phospholipase Cβ which in turn regulates calcium mobilisation and the activation of Protein kinase C (PKC), key mediators of granule secretion and activation of integrin $\alpha_{IIb}\beta_3$. $G_{\alpha 13}$ regulates the Rho/Rho-kinase signalling pathway which regulates the phosphorylation of myosin IIa and is important for the regulation of cytoskeletal rearrangements and platelet shape change.

To determine whether Pim kinase regulates processes downstream of TPαR coupled G proteins, levels of intracellular calcium, PKC activity and myosin light chain (MLC) phosphorylation were monitored following stimulation with U46619. As shown in figure 5B, treatment of platelets with AZD1208 caused a significant reduction in calcium mobilisation following stimulation with U46619 (0.3 μM) compared to vehicle control treated platelets. In contrast no significant difference in calcium mobilisation was observed following stimulation with ADP (10 μM) supporting a specific role for Pim kinase in the regulation of TPαR signalling. AZD1208 also caused a reduction both in PKC activity and MLC (S19) phosphorylation compared to vehicle controls following stimulation with U46619 (1μM) (Figure 5C and D). $G_{\alpha 13}$ is also associated with the regulation of integrin $\alpha_{IIb}\beta_3$ outside in signalling [25]. Phosphorylation of Y773 on the integrin β3 tail which is essential for propagation of outside-in signalling was reduced in U46619 stimulated platelets pretreated with AZD1208 compared to vehicle treated control platelets (Figure 5E). Taken together these results support a role for Pim kinase in the positive regulation of G_q and $G_{\alpha 13}$ signalling downstream of TPαR activation.

AZD1208 is not a competitive antagonist of the TPαR

As components of both G_q and G_{13} signalling, pathways immediately downstream of TPαR activation, were found to be inhibited following treatment with AZD1208 we hypothesised that it was having direct effect on the function of the TPαR itself. One potential mechanism of action could be that Pim kinase inhibitors such as AZD1208 act as antagonists of the TPαR and inhibit the TPαR directly, independent of Pim kinase. To determine whether AZD1208 acts as a competitive TPαR antagonist, platelet aggregation was measured following treatment with increasing concentrations of AZD1208 and stimulation with a range of U46619 concentrations so that the concentration relationship between inhibitor and antagonist could be quantified by Schild analysis. As shown in Figure 6A the inhibitory effect of AZD1208 became saturated by 10 µM, with higher concentrations (30, 50, 100 µM) unable to achieve greater levels of inhibition. In contrast, increasing concentrations of competitive TPαR antagonist GR32191 (Figure 5) caused non-saturable inhibition of aggregation stimulated by U46619 and generated a linear Schild plot with a pA2 of 8.9 which was consistent with the reported properties of this competitive antagonist acting at the TPαR [26] . In contrast, the Schild plot for AZD1208 was linear up to a concentration of 10 µM at which point the inhibitory effects were saturated and increasing concentrations AZD1208 no longer altered the apparent EC_{50} of U46619. These results indicate that the concentration-response relationship of GR32191 and U46619 in the aggregation assay was consistent with that of a TP receptor agonist and antagonist competing to bind to the orthosteric site, while the results with AZD1208 do not conform to this model.

AZD1208 alters TPαR receptor surface expression

It has been described previously that Pim kinase modulates levels of the CXCR4 receptor at the surface of CLL cells [18,19]. We hypothesised that Pim kinase inhibitors could modulate TPαR function via a similar mechanism in platelets and measured expression levels of TPαR following treatment with AZD1208 using flow cytometry to investigate this further. A TPαR antibody that recognises the N-terminal (extracellular) region of the TPαR was used to

determine surface expression levels of TPαR on platelets (Figure 6C). As previously described [27] stimulation of platelets with U46619 was associated with a reduction in cell surface levels of TPαR compared to unstimulated platelets due to receptor internalisation. Resting platelets treated with AZD1208 (10 μM) showed reduced surface levels of the TPαR receptor compared to vehicle treated controls with total levels of TPαR unaffected by AZD1208 treatment. U46619 (1 μM) stimulated platelets pretreated with AZD1208 also showed reduced surface expression levels of TPαR compared to vehicle treated controls and also compared platelets treated with U46619 only. These findings indicate that reduced U46619 signalling following treatment with AZD1208 is linked to reduced surface expression levels of TPαR.

AZD1208 inhibits CXCR4 signalling in human platelets

CXCR4 is expressed in platelets and is able to signal following stimulation with its ligand SDF-1α [28-30]. To determine whether inhibition of Pim kinase alters CXCR4 signalling in human platelets, aggregometry following stimulation with SDF-1α was performed in vehicle and AZD1208 treated human PRP, 200 ng/mL SDF-1α caused a modest level of platelet aggregation (~50%) in vehicle treated platelets which was significantly reduced in AZD1208 (100 μM) treated samples (~20% aggregation) (Figure 6D). These observations indicate that in addition to regulation of the TPαR, Pim kinase also regulates platelet CXCR4 receptor function.

DISCUSSION

Development of kinase inhibitors as potential therapeutics for solid tumours and haematological malignancies has been fuelled by the recent successes of kinase inhibitor therapy for cancers [1,2,31,32]. Pim kinase is known to enhance cancer progression and drug resistance, and loss of all three Pim kinase isoforms does not affect embryo viability, indicating inhibition of Pim activity is likely to be tolerable [10,11,33]. In addition to its well established role in the regulation of cycle progression and prevention of cellular apoptosis [3-6,23], it has also been shown to play roles in cell migration, potentially contributing to metastasis and cell invasion

[18,19] and is also implicated in drug resistance through activation of multi-drug resistance transporters [7-9]. Pim kinase and is therefore seen as a promising potential drug target.

Pim kinases have been shown to be highly expressed in hematopoietic cells with important roles in the development and differentiation of megakaryocytes [10] and platelets [11 15]. Deletion Pim-1 alone has no effect on the hematopoietic system [16], possibly indicating a level of redundancy between the Pim kinase family members. Kinases often have broad expression profiles across several different cell types which increases the risk of kinase inhibitors having unwanted side effects. Platelets in particular rely heavily on kinase driven signalling cascades to enable them to function effectively in response to vascular damage. Several kinase inhibitors have been reported that affect the ability of platelets to activate and are associated with an increased risk of bleeding [34 35,36].

Western blot analysis identified expression of both the 44 kDa and 32 kDa variants of Pim-1 kinase in human and mouse platelets. Whilst Pim-2 and Pim-3 were not identified in our assays, expression of either paralog in human and mouse platelets cannot be ruled out. Comparison of thrombus formation on collagen under flow *in vitro* established that platelets from Pim-1 deficient mice showed significant attenuation in comparison to wild type control, highlighting a role for Pim-1 kinase in the regulation of platelet function and thrombus formation under arterial flow on collagen. Despite the reduction in thrombotic potential, deletion of Pim-1 was not associated with altered haemostasis, indicating that drugs targeting Pim kinase activity could offer an anti-thrombotic therapeutic strategy that is not associated with increased bleeding risk usually observed with other anti-platelet agents.

In support of the anti-thrombotic potential of Pim kinase inhibitors we determined that several structurally different Pim kinase inhibitors AZD1208, PIM-447, SGI-1776, SMI-4a and CX6258, which are pan-Pim kinase inhibitors that target all three Pim kinases, all caused inhibition of platelet functional responses, including aggregation to GPVI agonists collagen and CRP-XL, CXCR4 ligand SDF-1α (CXCL12) and TxA_2 mimetic U46619, but not to other GPCR agonists including thrombin, TRAP6 or ADP, with an inhibitory profile similar to that

observed by Lordkipanidzé *et al* in a patient with a mutation in the TP receptor [27,37]. Furthermore inhibition of collagen induced platelet responses was found to be due to an inhibition of TPαR signalling as the level of platelet aggregation observed in the presence of indomethacin or TPαR antagonist GR32191 was not further decreased following treatment with AZD1208 (10µM). Similar to the reduced thrombus formation observed in whole blood from Pim-1 deficient mice, AZD1208 caused significant attenuation of thrombus formation on collagen under flow *in vitro* under arterial and pathological shear rates and dramatic inhibition of thrombus formation *in vivo* (Figure 2). Interestingly however, no effect on platelet adhesion and thrombus formation at venous flow rates was observed following treatment with AZD1208, this combined with the lack of effect on bleeding in mice following damage to the tail vein, suggests that although Pim kinase inhibition or deficiency reduces thrombus formation under high arterial shear, this does not alter thrombus formation or haemostasis at venous or low shear. This absence of effect is likely due to the lack of inhibition of PAR or P2Y receptor mediated platelet activation by Pim kinase inhibitors. Previous studies have shown that whilst GPVI deficiency or inhibition has varying effects in tail bleeding assays[38 39], PAR or $P2Y_{12}$ deficiency or $P2Y_1$ inhibition results in significant increases in tail bleeding and alteration of haemostasis in mice [39-41]. As initial adhesion to collagen is unaffected following treatment with AZD1208, maintenance of PAR and P2Y receptor responses may compensate for the lack of TP receptor signalling allowing for normal haemostasis. The lack of bleeding effect following treatment with AZD1208 is consistent with the lack of reported bleeding related adverse effects in patients in a recent phase 1 clinical study investigating the efficacy of AZD1208 in solid and haematological cancers [24]. This provides further evidence that Pim kinase inhibitors may not be associated with drug induced platelet dysfunction related bleeding events and points to future use of Pim kinase inhibitors as a possible treatment strategy for individuals with increased risk of CVD and atherosclerosis, conditions associated with pathological shear rates.

Investigation into how Pim kinases elicit their inhibitory effects on TPαR signalling, revealed that AZD1208 inhibited TPαR downstream signalling events pointing to upstream regulation of TPαR signalling most likely via direct regulation of the TPαR. It has previously been described that Pim- 1 kinase regulates CXCR4 activity in Jurkat and CLL cells via regulation of receptor surface expression levels of the receptor [18,19]. Inhibition or deletion of Pim kinase reduces surface expression levels of CXCR4 and inhibits CXCL12/SDF-1 signalling [29,30]. Similarly, in our study we identified reduced surface expression levels of the TPαR in platelets following treatment with AZD1208 compared to vehicle treated controls.

The TPαR signalling pathway is a key target to reduce CVD related thrombotic events and inflammation in patients. Despite widespread use, currently available GPCR targeted therapies are associated with variable patient outcomes and adverse side effects. Aspirin is the 'gold standard' anti-platelet agent for the prevention of arterial thrombosis. Aspirin targets platelet TPαR signalling via an indirect route, by inhibiting COX-1, the enzyme that controls synthesis of TxA_2. Aspirin however, has dose-limiting off-target effects on COX-2, an enzyme involved in synthesis of endogenous inhibitors of platelet function that can increase the risk of thrombosis when repressed. Aspirin is also less effective in patients suffering from diabetes, hypertension and obesity, and is associated with increased severe bleeding risk [42] with one recent meta-analyses suggesting that in low risk individuals the harms of aspirin outweighs the cardiovascular benefits [43,44] [45].Our findings suggest that Pim kinases may be a safer target to control thrombosis.

The mechanism underlying the regulation of TPαR signalling by Pim-1 kinase requires further investigation. In other cell types the 44 kDa variant of Pim-1 kinase, Pim-1L is localised to the plasma membrane and associated with the phosphorylation and regulation of several membrane proteins, whilst the smaller 32 kDa variant Pim-1S predominantly localises to the cytosol and nucleus [7,46]. One possibility is that Pim kinase phosphorylates the TPαR controlling its surface expression levels, similar to the mechanism observed for CXCR4 in CLL cells. Sequence alignments of the Pim kinase substrate recognition sequence have identified 4

putative Pim kinase phosphorylation sites within the TPαR sequence including one within the first intracellular loop, a region that has previously been shown to be associated with TPαR surface expression and receptor function [27]. Pim kinase inhibition may therefore disrupt phosphorylation of the receptor and reduce surface expression via increasing its internalisation or preventing the dynamic process of receptor recycling to the surface. It is also possible that Pim kinase does not phosphorylate the receptor directly and instead orchestrates interaction with other proteins that regulate receptor surface expression [18,19].

This work identifies a novel, Pim kinase dependent regulatory mechanism for the TPαR and represents a new targeting strategy that is independent of COX-1 inhibition or direct antagonism of the TPαR that whilst reducing thrombosis does not increase the risk of bleeding.

AUTHOR CONTRIBUTIONS

Contribution: A.J.U designed the research, performed experiments and analysed results and wrote the paper, A.P.B. T.S, R.S.G, N.E, C.D, A.S, N.K, P.J.V, L.H, R.R, S.J, S.M and W.C performed experiments and analysed results. H.F, J.M.G designed the research and wrote the paper.

ACKNOWLEDGEMENTS

The authors would like to thank Gemma Little, Joanne Mitchell and Mike Fry, University of Reading for their help with work and the preparation of this manuscript.

SOURCES OF FUNDING

This work was supported by the British Heart Foundation programme grant RG/15/2/31224 (J.M.G), National Institutes of Health R01 grants HL126743 (H.F) and AI125741 (W.C), the Centre for Biosciences, Manchester Metropolitan University and Manchester Metropolitan University RKE Internal Funding grant 343846 (A.U).

REFERENCES

1. Pogacic V, Bullock AN, Fedorov O, et al. Structural analysis identifies imidazo[1,2-b]pyridazines as PIM kinase inhibitors with in vitro antileukemic activity. *Cancer Res.* 2007;67(14):6916-6924.
2. Shah N, Pang B, Yeoh KG, et al. Potential roles for the PIM1 kinase in human cancer - a molecular and therapeutic appraisal. *Eur J Cancer.* 2008;44(15):2144-2151.
3. Bachmann M, Moroy T. The serine/threonine kinase Pim-1. *Int J Biochem Cell Biol.* 2005;37(4):726-730.
4. Bachmann M, Kosan C, Xing PX, Montenarh M, Hoffmann I, Moroy T. The oncogenic serine/threonine kinase Pim-1 directly phosphorylates and activates the G2/M specific phosphatase Cdc25C. *Int J Biochem Cell Biol.* 2006;38(3):430-443.
5. Macdonald A, Campbell DG, Toth R, McLauchlan H, Hastie CJ, Arthur JS. Pim kinases phosphorylate multiple sites on Bad and promote 14-3-3 binding and dissociation from Bcl-XL. *BMC Cell Biol.* 2006;7:1.
6. Aho TL, Sandholm J, Peltola KJ, Mankonen HP, Lilly M, Koskinen PJ. Pim-1 kinase promotes inactivation of the pro-apoptotic Bad protein by phosphorylating it on the Ser112 gatekeeper site. *FEBS Lett.* 2004;571(1-3):43-49.
7. Xie Y, Xu K, Linn DE, et al. The 44-kDa Pim-1 kinase phosphorylates BCRP/ABCG2 and thereby promotes its multimerization and drug-resistant activity in human prostate cancer cells. *J Biol Chem.* 2008;283(6):3349-3356.
8. Darby RA, Unsworth A, Knapp S, Kerr ID, Callaghan R. Overcoming ABCG2-mediated drug resistance with imidazo-[1,2-b]-pyridazine-based Pim1 kinase inhibitors. *Cancer Chemother Pharmacol.* 2015;76(4):853-864.
9. Xie Y, Burcu M, Linn DE, Qiu Y, Baer MR. Pim-1 kinase protects P-glycoprotein from degradation and enables its glycosylation and cell surface expression. *Mol Pharmacol.* 2010;78(2):310-318.
10. Mikkers H, Nawijn M, Allen J, et al. Mice deficient for all PIM kinases display reduced body size and impaired responses to hematopoietic growth factors. *Mol Cell Biol.* 2004;24(13):6104-6115.
11. An N, Kraft AS, Kang Y. Abnormal hematopoietic phenotypes in Pim kinase triple knockout mice. *J Hematol Oncol.* 2013;6:12.
12. Senis YA, Tomlinson MG, Garcia A, et al. A comprehensive proteomics and genomics analysis reveals novel transmembrane proteins in human platelets and mouse megakaryocytes including G6b-B, a novel immunoreceptor tyrosine-based inhibitory motif protein. *Mol Cell Proteomics.* 2007;6(3):548-564.
13. Weyrich AS, Zimmerman GA. Evaluating the relevance of the platelet transcriptome. *Blood.* 2003;102(4):1550-1551.
14. Rowley JW, Oler AJ, Tolley ND, et al. Genome-wide RNA-seq analysis of human and mouse platelet transcriptomes. *Blood.* 2011;118(14):e101-111.
15. An N, Lin YW, Mahajan S, et al. Pim1 serine/threonine kinase regulates the number and functions of murine hematopoietic stem cells. *Stem Cells.* 2013;31(6):1202-1212.
16. Laird PW, van der Lugt NM, Clarke A, et al. In vivo analysis of Pim-1 deficiency. *Nucleic Acids Res.* 1993;21(20):4750-4755.
17. Li D, D'Angelo L, Chavez M, Woulfe DS. Arrestin-2 differentially regulates PAR4 and ADP receptor signaling in platelets. *J Biol Chem.* 2011;286(5):3805-3814.
18. Grundler R, Brault L, Gasser C, et al. Dissection of PIM serine/threonine kinases in FLT3-ITD-induced leukemogenesis reveals PIM1 as regulator of CXCL12-CXCR4-mediated homing and migration. *J Exp Med.* 2009;206(9):1957-1970.
19. Decker S, Finter J, Forde AJ, et al. PIM kinases are essential for chronic lymphocytic leukemia cell survival (PIM2/3) and CXCR4-mediated microenvironmental interactions (PIM1). *Mol Cancer Ther.* 2014;13(5):1231-1245.
20. Watkins NA, Gusnanto A, de Bono B, et al. A HaemAtlas: characterizing gene expression in differentiated human blood cells. *Blood.* 2009;113(19):e1-9.

21. Simon LM, Edelstein LC, Nagalla S, et al. Human platelet microRNA-mRNA networks associated with age and gender revealed by integrated plateletomics. *Blood.* 2014;123(16):e37-45.
22. Lin YW, Beharry ZM, Hill EG, et al. A small molecule inhibitor of Pim protein kinases blocks the growth of precursor T-cell lymphoblastic leukemia/lymphoma. *Blood.* 2010;115(4):824-833.
23. Yan B, Zemskova M, Holder S, et al. The PIM-2 kinase phosphorylates BAD on serine 112 and reverses BAD-induced cell death. *J Biol Chem.* 2003;278(46):45358-45367.
24. Cortes J, Tamura K, DeAngelo DJ, et al. Phase I studies of AZD1208, a proviral integration Moloney virus kinase inhibitor in solid and haematological cancers. *Br J Cancer.* 2018;118(11):1425-1433.
25. Gong H, Shen B, Flevaris P, et al. G protein subunit Galpha13 binds to integrin alphaIIbbeta3 and mediates integrin "outside-in" signaling. *Science.* 2010;327(5963):340-343.
26. Lumley P, White BP, Humphrey PP. GR32191, a highly potent and specific thromboxane A2 receptor blocking drug on platelets and vascular and airways smooth muscle in vitro. *Br J Pharmacol.* 1989;97(3):783-794.
27. Nisar SP, Lordkipanidze M, Jones ML, et al. A novel thromboxane A2 receptor N42S variant results in reduced surface expression and platelet dysfunction. *Thromb Haemost.* 2014;111(5):923-932.
28. Akbiyik F, Ray DM, Gettings KF, Blumberg N, Francis CW, Phipps RP. Human bone marrow megakaryocytes and platelets express PPARgamma, and PPARgamma agonists blunt platelet release of CD40 ligand and thromboxanes. *Blood.* 2004;104(5):1361-1368.
29. Walsh TG, Harper MT, Poole AW. SDF-1alpha is a novel autocrine activator of platelets operating through its receptor CXCR4. *Cell Signal.* 2015;27(1):37-46.
30. Clemetson KJ, Clemetson JM, Proudfoot AE, Power CA, Baggiolini M, Wells TN. Functional expression of CCR1, CCR3, CCR4, and CXCR4 chemokine receptors on human platelets. *Blood.* 2000;96(13):4046-4054.
31. Keeton EK, McEachern K, Dillman KS, et al. AZD1208, a potent and selective pan-Pim kinase inhibitor, demonstrates efficacy in preclinical models of acute myeloid leukemia. *Blood.* 2014;123(6):905-913.
32. Kirschner AN, Wang J, van der Meer R, et al. PIM kinase inhibitor AZD1208 for treatment of MYC-driven prostate cancer. *J Natl Cancer Inst.* 2015;107(2).
33. Din S, Konstandin MH, Johnson B, et al. Metabolic dysfunction consistent with premature aging results from deletion of Pim kinases. *Circ Res.* 2014;115(3):376-387.
34. Bye AP, Unsworth AJ, Vaiyapuri S, Stainer AR, Fry MJ, Gibbins JM. Ibrutinib Inhibits Platelet Integrin alphaIIbbeta3 Outside-In Signaling and Thrombus Stability But Not Adhesion to Collagen. *Arteriosclerosis, thrombosis, and vascular biology.* 2015.
35. Gratacap MP, Martin V, Valera MC, et al. The new tyrosine-kinase inhibitor and anticancer drug dasatinib reversibly affects platelet activation in vitro and in vivo. *Blood.* 2009;114(9):1884-1892.
36. Levade M, Severin S, Gratacap MP, Ysebaert L, Payrastre B. Targeting Kinases in Cancer Therapies: Adverse Effects on Blood Platelets. *Curr Pharm Des.* 2016;22(16):2315-2322.
37. Lordkipanidze M, Lowe GC, Kirkby NS, et al. Characterization of multiple platelet activation pathways in patients with bleeding as a high-throughput screening option: use of 96-well Optimul assay. *Blood.* 2014;123(8):e11-22.
38. Nieswandt B, Watson SP. Platelet-collagen interaction: is GPVI the central receptor? *Blood.* 2003;102(2):449-461.
39. Bynagari-Settipalli YS, Cornelissen I, Palmer D, et al. Redundancy and interaction of thrombin- and collagen-mediated platelet activation in tail bleeding and carotid thrombosis in mice. *Arterioscler Thromb Vasc Biol.* 2014;34(12):2563-2569.
40. Dorsam RT, Kunapuli SP. Central role of the P2Y12 receptor in platelet activation. *J Clin Invest.* 2004;113(3):340-345.

41. Karim ZA, Vemana HP, Alshbool FZ, et al. Characterization of a novel function-blocking antibody targeted against the platelet P2Y1 receptor. *Arterioscler Thromb Vasc Biol.* 2015;35(3):637-644.
42. Hankey GJ, Eikelboom JW. Aspirin resistance. *Lancet.* 2006;367(9510):606-617.
43. Warner TD, Nylander S, Whatling C. Anti-platelet therapy: cyclo-oxygenase inhibition and the use of aspirin with particular regard to dual anti-platelet therapy. *Br J Clin Pharmacol.* 2011;72(4):619-633.
44. Desborough MJR, Keeling DM. The aspirin story - from willow to wonder drug. *Br J Haematol.* 2017;177(5):674-683.
45. Antithrombotic Trialists C, Baigent C, Blackwell L, et al. Aspirin in the primary and secondary prevention of vascular disease: collaborative meta-analysis of individual participant data from randomised trials. *Lancet.* 2009;373(9678):1849-1860.
46. Xie Y, Xu K, Dai B, et al. The 44 kDa Pim-1 kinase directly interacts with tyrosine kinase Etk/BMX and protects human prostate cancer cells from apoptosis induced by chemotherapeutic drugs. *Oncogene.* 2006;25(1):70-78.

FIGURE LEGENDS

Figure 1. Expression of Pim kinase in human and mouse platelets. A i) HaemAtlas analysis of Pim kinase mRNA expression levels. Pim kinase mRNA levels were quantified in human megakaryocytes and a range of blood cells by analysis of gene array data. Megakaryocytes (MK), human erythroblasts (EB), HUVEC cells, monocytes (CD14), granulocytes (CD66), mature B cells (CD19), natural killer cells (CD56), cytotoxic T cells (CD*) and helper T cells (CD4), 10+ (lighter colour) was deemed high expression. B) Human and mouse washed platelets (three preparations) were lysed in SDS PAGE Laemmli sample buffer, separated on SDS PAGE gels and transferred to PVDF membranes before blotting with anti-Pim-1 antibody. K562 and Jurkat cell lysates were included as positive controls. Actin was included as a loading control. Representative blots shown.

Figure 2. Genetic deletion and pharmacological inhibition of Pim-1 kinase attenuates thrombus formation on collagen, but does not cause bleeding. A) DiOC6 loaded mouse whole blood from Pim1$^{+/-}$ (black) or Pim1$^{-/-}$ (red) mice was perfused through collagen coated (100 µg/mL) Vena8Biochips at a shear rate of 1500 s^{-1}. i) Representative images taken at the end of recording shown. ii) Thrombus formation was determined after 4 minutes by comparing % area covered. B) Tail bleeding in Pim-1$^{+/-}$ or Pim-1$^{-/-}$ mice represented as time to cessation of bleeding (secs). C, D and E) DiOC6 loaded human whole blood was pretreated with vehicle (black) or 100 µM AZD1208 (red) for 10 minutes before perfusion through collagen coated (100 µg/mL) Vena8Biochips at a C) arterial shear rate of 20 dyn/cm^2, D) pathological shear rate of 135 dyn/cm^2 or E) venous shear rate of 4.5 dyn cm^2, 100µM AZD1208 was chosen due to reduced bioavailability of AZD1208 in plasma. Thrombus formation was determined after 5 (pathological shear) or 10 (arterial and venous) minutes by comparing % max vehicle

fluorescence intensity, which measures both surface area coverage and thrombus size, in the vehicle and treated samples. i) Representative images taken at the end of recording shown. ii) Data expressed as % max vehicle fluorescence intensity. F) Thrombus formation was determined in vivo following FeCl3 injury in mice pretreated for 10 mins with vehicle or 100 µM AZD1208, DiOC6 used to enable visualisation of platelets, i) representativs images taken at 0,. 300, 600 and 900 secs, ii) Data expressed as time to occlusion (secs). (G) Tail bleeding determined as time to cessation of bleeding (secs) in mice pretreated with vehicle or 100 µM AZD1208 for 10 minutes. Results are mean ± S.E.M. for n≥3, * indicates p≤0.05 ** indicates p≤0.01 **** indicates p≤0.001 in comparison to vehicle control, where normalised data shown, statistics were performed prior to normalisation.

Figure 3. AZD1208 inhibits platelet aggregation. Washed human platelets were pre-treated with increasing concentrations of AZD1208 (0.1, 1, 10 µM) prior to stimulation with either A) Collagen (1 µg/mL), B) CRP-XL (0.3 µg/mL), C) U46619 (0.3 µM), D) Thrombin (0.03 U/mL) and E) ADP (10 µM) and aggregation monitored using optical light transmission aggregometry, i) Representative traces and ii) quantified data shown. iii) Human washed platelets were pre-treated with 10 µM AZD1208 (red) or vehicle (black) prior to stimulation with A) collagen (0.01-10 µg/mL), B) CRP-XL (1-3 µg/mL), C) U46619 (3 nM- 3µM), D) Thrombin (0.01-1 U/mL) or E) ADP (0.1-100 µM) and aggregation was monitored after 5 minutes using an optical light transmission plate based aggregometry assay, quantified data shown. Results are mean ± S.E.M. for n≥3, * indicates p≤0.05 *** indicates p≤0.005 in comparison to vehicle control; where normalised data shown, statistics were performed prior to normalisation.

Figure 4. Inhibition of thromboxane A2 signalling underlies inhibition of collagen induced aggregation and thrombus formation by Pim kinase inhibitors. Human washed platelets were treated with A) increasing concentrations of AZD1208 (1-100 µM) or vehicle control prior to stimulation with increasing concentrations of U46619 (0.03 – 10 µM). B) 10 µM AZD1208 in the presence or absence of A) indomethacin (10 µM) or B) TxA2 receptor antagonist GR32191 (100 nM) and aggregation monitored after 5 minutes of stimulation by collagen (0.01-10 µg/mL) using a 96 well plate based aggregometry assay. C) DiOC6 loaded human whole blood was pretreated with vehicle (black) or 100 µM AZD1208 (red), in the presence of 10 µM indomethacin for 10 minutes before perfusion through collagen coated (100 µg/mL) Vena8Biochips at a shear rate of 20 dyn/cm^2. Thrombus formation was determined over 10 minutes by comparing fluorescence intensity in the vehicle and treated samples. i) Representative images taken at 10 minutes shown. ii) Data expressed as % max vehicle fluorescence and normalised to an untreated (no indomethacin treatment) control, where the maximum fluorescence observed in untreated platelets is considered to be 100%

thrombus formation. D) Fibrinogen binding in mouse washed platelets from control (Pim1 +/-) or Pim1-/- mice was determined following stimulation with Thrombin (0.01 U/mL), U46619 (10 µM) and CRP (10 µg/mL) and expressed as % positive cells. Results are mean + S.E.M. for n≥3, * indicates p≤0.05 ***p≤0.005 in comparison to vehicle control; where normalised data shown, statistics were performed prior to normalisation.

Figure 5. AZD1208 inhibits TP receptor signalling. Resting and stimulated human washed platelets were treated with 10 µM AZD1208 for 10 minutes and A) stimulated with i) collagen (1 µg/mL) or arachidonic acid (1 mM) or ii) U46619 (0-3µM) in the presence and absence of indomethacin (10 µM) and i) TxB2 levels (EnzoLife sciences ELISA) or ii) aggregation monitored after five minutes of shaking. B) Mobilisation of intracellular calcium was determined in FURA-2 AM loaded platelets following stimulation with U46619 (300 nM) or ADP (10 µM) i) Representative traces and ii) quantified data shown and data expressed as the change in $[Ca^{2+}]$ (nM) C-E) Human platelets were pre-incubated with vehicle or AZD1208 (10 µM) for 10 minutes and stimulated with U46619 (1 µM) for 30 secs or 3 minutes before lysis in SDS Laemmli sample buffer C) PKC activity was determined by blotting these samples and using a phospho-site specific antibody (for the PKC substrate recognition sequence) which detects PKC substrate phosphorylation and D) myosin light chain phosphorylation at Ser19 using a phospho-specific antibody (that recognises the phosphorylated myosin light chain). E) phosphorylation of the integrin β3 subunit at Y773 using a phospho-specific antibody. Actin was used to confirm equal loading. i) representative blots and ii) quantified data shown. Levels of total phosphorylation were quantified and expressed as a percentage of the maximum phosphorylation observed in vehicle treated stimulated controls. Results are mean + S.E.M. for n≥3, * indicates p≤0.05 in comparison to vehicle controls.

Figure 6. AZD1208 reduces TPαR surface expression and signalling and does not act as a competitive antagonist of the TPαR. Human washed platelets were pre-treated with A) AZD1208 (1, 3, 10, 30, 50 and 100 µM) or B) GR32191 (1, 2, 3, 5, 10, 30, 100 nM) prior to stimulation with U46619 (3 nM- 3µM) and aggregation was monitored after 5 minutes using an optical light transmission plate based aggregometry assay, quantified data shown. i) percentage aggregation. ii) EC50 values from the aggregation dose response curves determined following incubation with AZD1208 were used to plot a Schild regression plot to determine whether AZD1208 acts as an antagonist for the TxA_2 receptor. C) AZD1208 (10 µM; 10 mins) or vehicle control and ii) surface expression of TPαR was assessed using an antibody that recognises the extracellular portion of the TPαR and detected by flow cytometry. Samples were diluted in HBS and not fixed to avoid disruption of the membrane. Anti-DOK6 antibody was included as a negative control. i) shows a representative histogram from the flow

cytometer. ii) Data expressed as a median fluorescent intensity. iii) Total cellular TPαR was detected by western blotting. D) Human PRP was pre-treated with AZD1208 (100 μM) or vehicle control for 10 minutes prior to stimulation with SDF-1α (200 ng/mL) and aggregation monitored using optical light transmission aggregometry for 5 minutes. i) Representative trace and ii) quantified data shown. Results are mean + S.E.M. for n≥3, * indicates p≤0.05 ** indicates p≤0.01 *** indicates p≤0.005 in comparison to vehicle control, where normalised data shown, statistics were performed prior to normalisation.

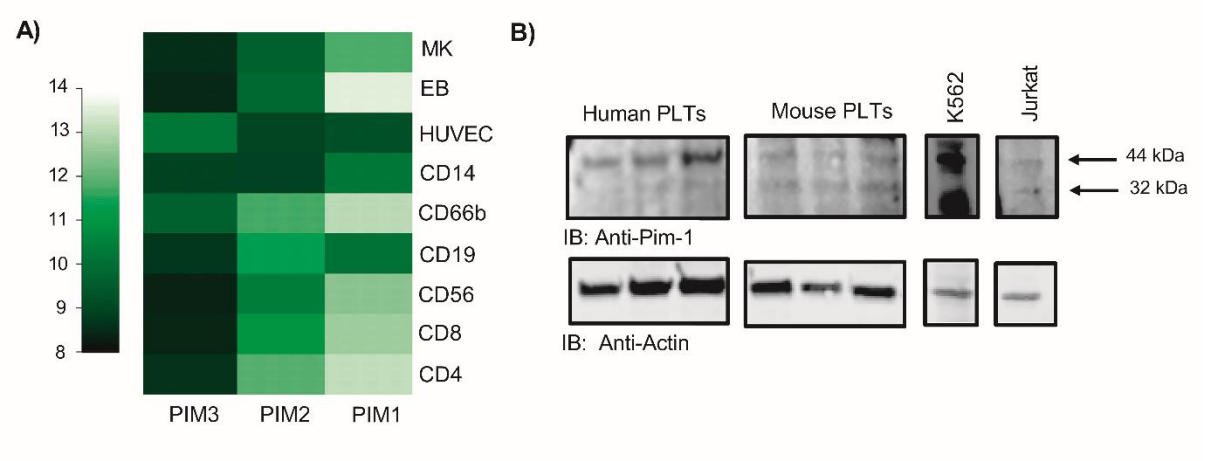
A)
14
13
12
11
10
9
8
MK
EB
HUVEC
CD14
CD66b
CD19
CD56
CD8
CD4
PIM3
PIM2
PIM1
B)
Human PLTs
Mouse PLTs
K562
Jurkat
44 kDa
32 kDa
IB: Anti-Pim-1
IB: Anti-Actin

Figure 1

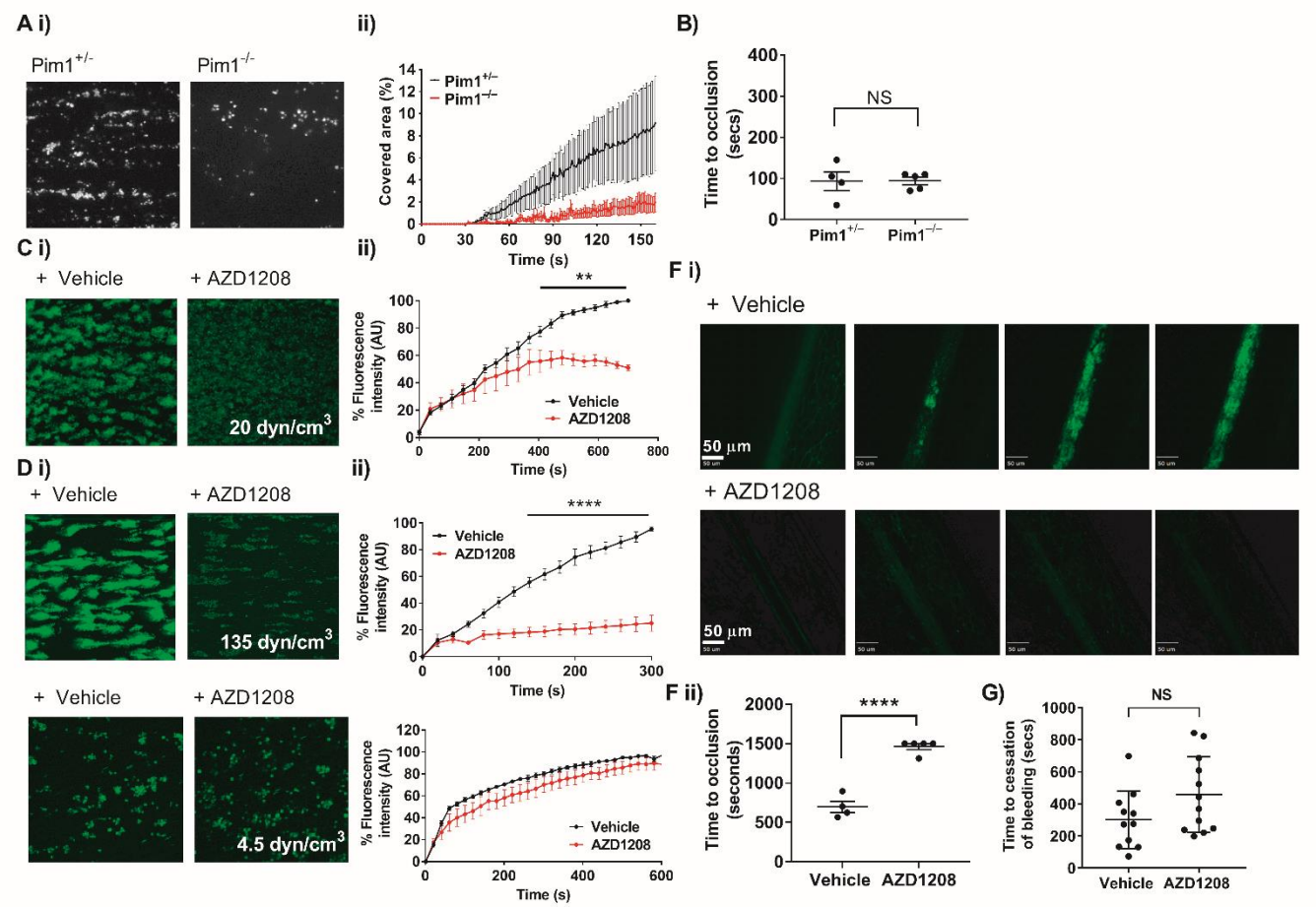
A i)
Pim1+/-
Pim1-/-
ii)
Covered area (%)
Pim1+/-
Pim1-/-
Time (s)
B)
Time to occlusion (secs)
NS
Pim1+/-
Pim1-/-
C i)
+ Vehicle
+ AZD1208
20 dyn/cm3
ii)
% Fluorescence intensity (AU)
**
Vehicle
AZD1208
Time (s)
D i)
+ Vehicle
+ AZD1208
135 dyn/cm3
ii)
% Fluorescence intensity (AU)
****
Vehicle
AZD1208
Time (s)
+ Vehicle
+ AZD1208
4.5 dyn/cm3
% Fluorescence intensity (AU)
Vehicle
AZD1208
Time (s)
F i)
+ Vehicle
50 µm
+ AZD1208
50 µm
F ii)
Time to occlusion (seconds)
****
Vehicle
AZD1208
G)
Time to cessation of bleeding (secs)
NS
Vehicle
AZD1208

Figure 2

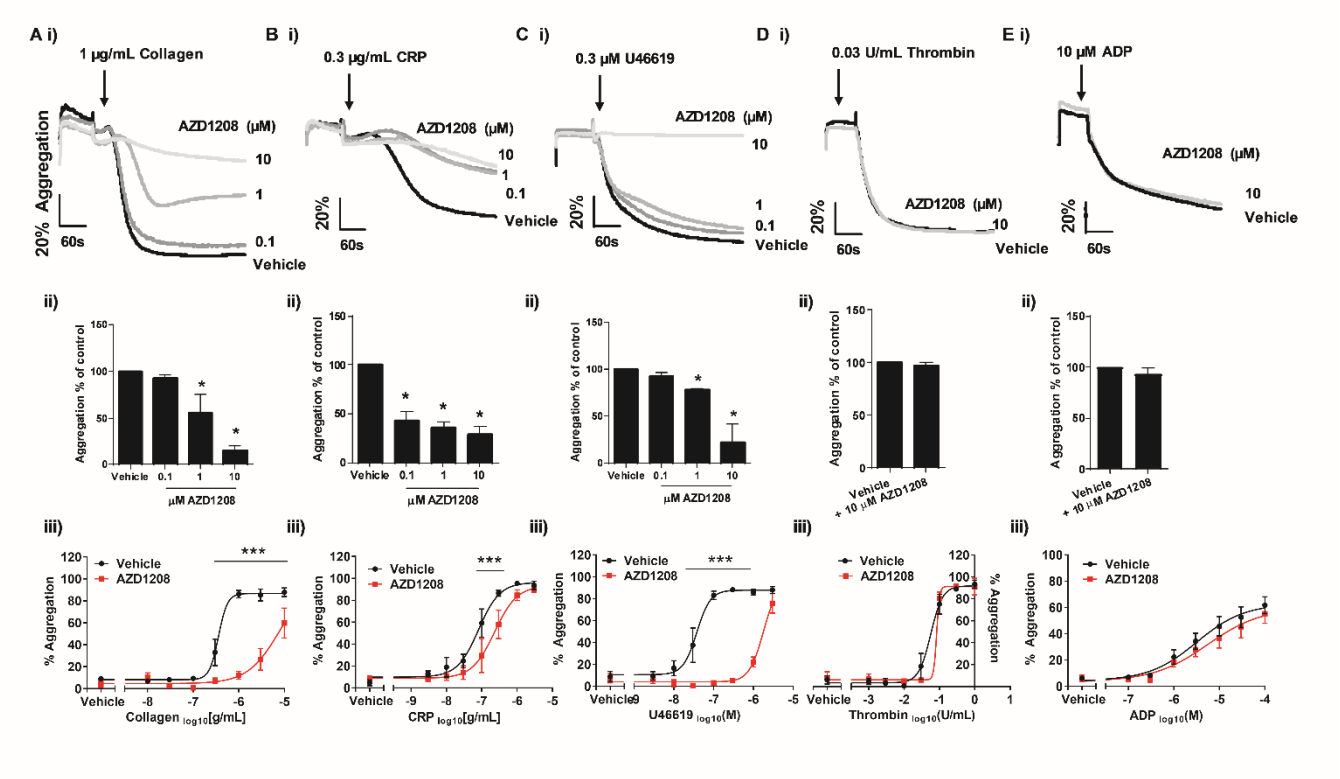
A i)
1 µg/mL Collagen
AZD1208 (µM)
10
1
0.1
Vehicle
20% Aggregation
60s
B i)
0.3 µg/mL CRP
AZD1208 (µM)
10
1
0.1
Vehicle
20%
60s
C i)
0.3 µM U46619
AZD1208 (µM)
10
1
0.1
Vehicle
20%
60s
D i)
0.03 U/mL Thrombin
AZD1208 (µM)
10
Vehicle
20%
60s
E i)
10 µM ADP
AZD1208 (µM)
10
Vehicle
20%
60s
ii)
Aggregation % of control
Vehicle
0.1
1
10
µM AZD1208
Vehicle
10 µM AZD1208
iii)
Vehicle
AZD1208
***
% Aggregation
Collagen log10[g/mL]
CRP log10[g/mL]
U46619 log10(M)
Thrombin log10(U/mL)
ADP log10(M)

Figure 3

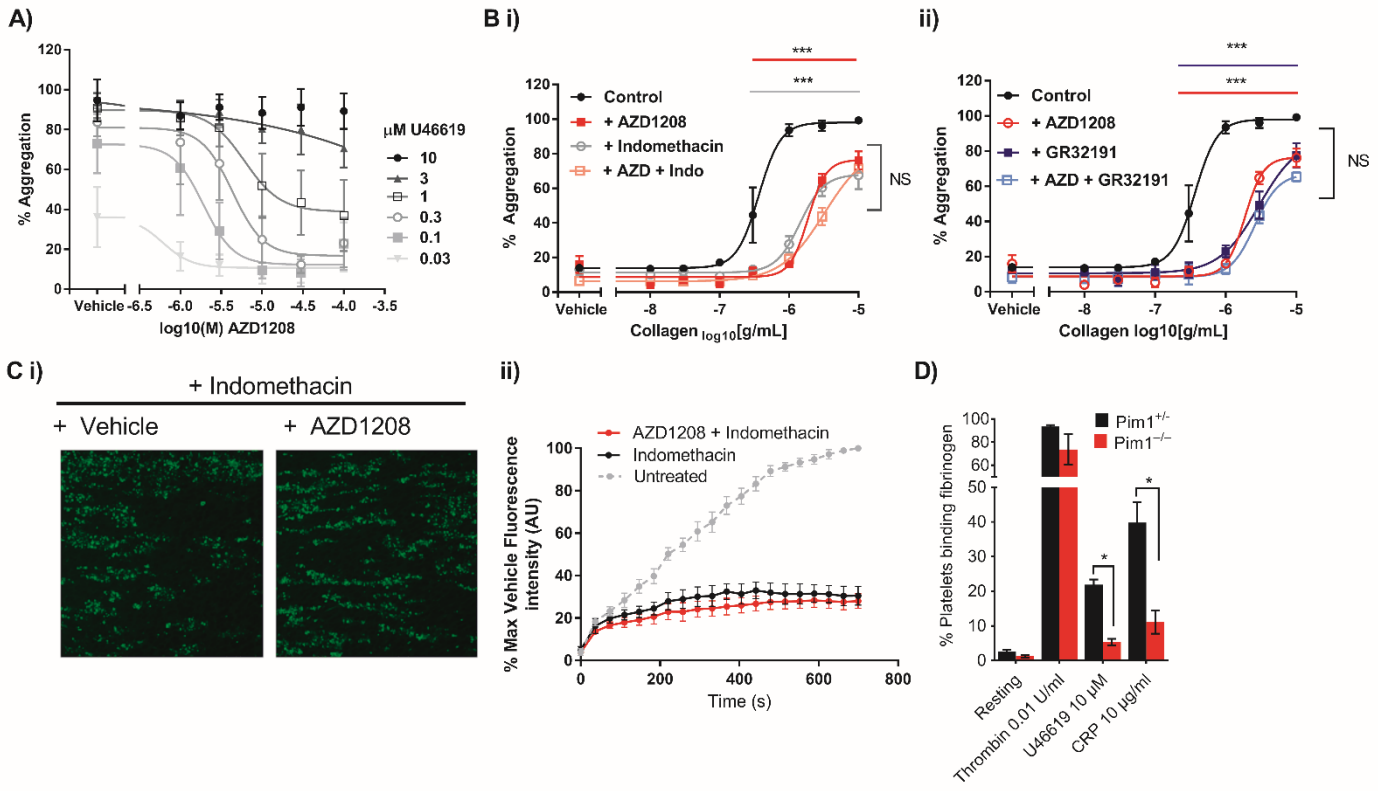
A)
% Aggregation
μM U46619
10
3
1
0.3
0.1
0.03
Vehicle -6.5 -6.0 -5.5 -5.0 -4.5 -4.0 -3.5
log10(M) AZD1208
B i)
Control
+ AZD1208
+ Indomethacin
+ AZD + Indo
***
***
NS
Vehicle -8 -7 -6 -5
Collagen log10[g/mL]
ii)
Control
+ AZD1208
+ GR32191
+ AZD + GR32191
***
***
NS
Vehicle -8 -7 -6 -5
Collagen log10[g/mL]
C i)
+ Indomethacin
+ Vehicle
+ AZD1208
ii)
AZD1208 + Indomethacin
Indomethacin
Untreated
% Max Vehicle Fluorescence intensity (AU)
Time (s)
D)
Pim1+/-
Pim1-/-
% Platelets binding fibrinogen
Resting
Thrombin 0.01 U/ml
U46619 10 μM
CRP 10 μg/ml

Figure 4

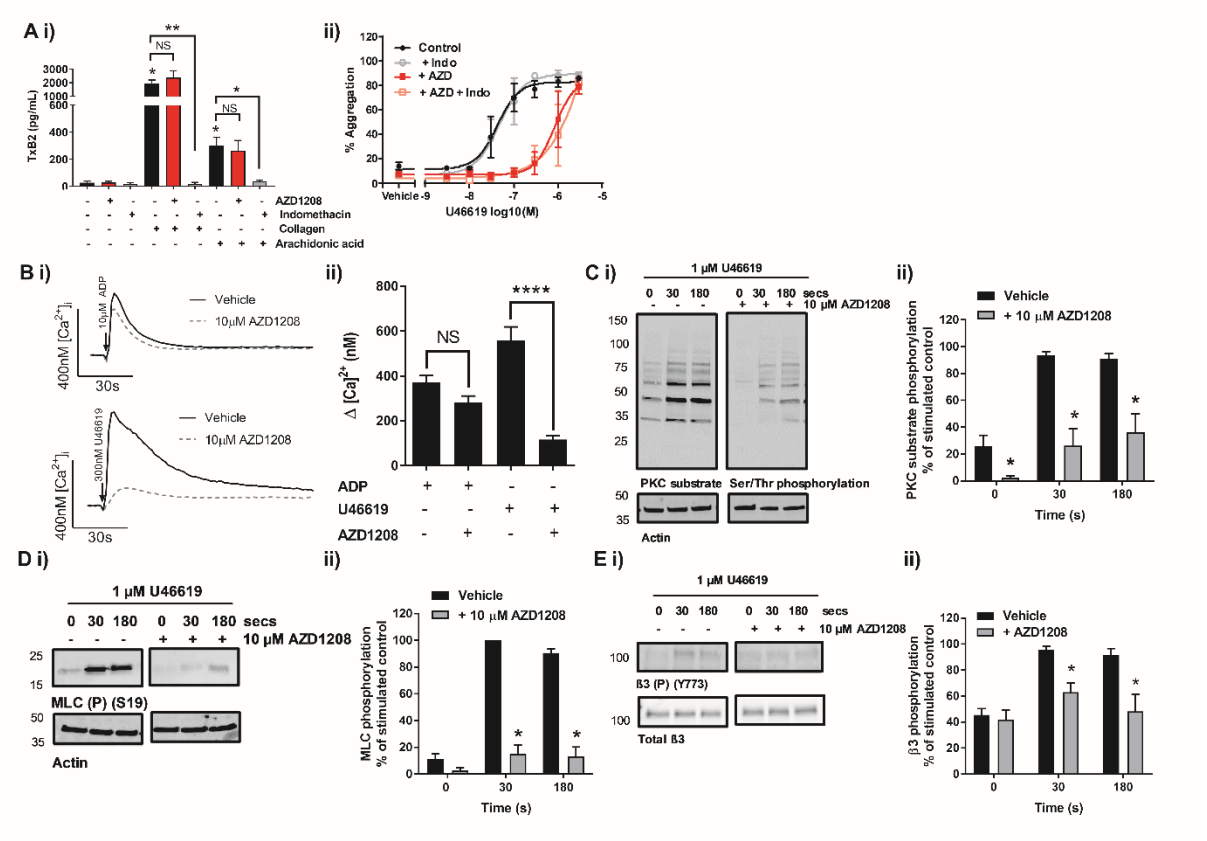
A i)
TxB2 (pg/mL)
AZD1208
Indomethacin
Collagen
Arachidonic acid
ii)
% Aggregation
Control
+ Indo
+ AZD
+ AZD + Indo
U46619 log10(M)
B i)
Vehicle
10μM AZD1208
400nM [Ca2+]i
30s
ii)
Δ [Ca]2+ (nM)
ADP
U46619
AZD1208
C i)
1 μM U46619
10 μM AZD1208
PKC substrate
Ser/Thr phosphorylation
Actin
ii)
PKC substrate phosphorylation % of stimulated control
Time (s)
D i)
MLC (P) (S19)
Actin
ii)
MLC phosphorylation % of stimulated control
E i)
ß3 (P) (Y773)
Total ß3
ii)
ß3 phosphorylation % of stimulated control

Figure 5

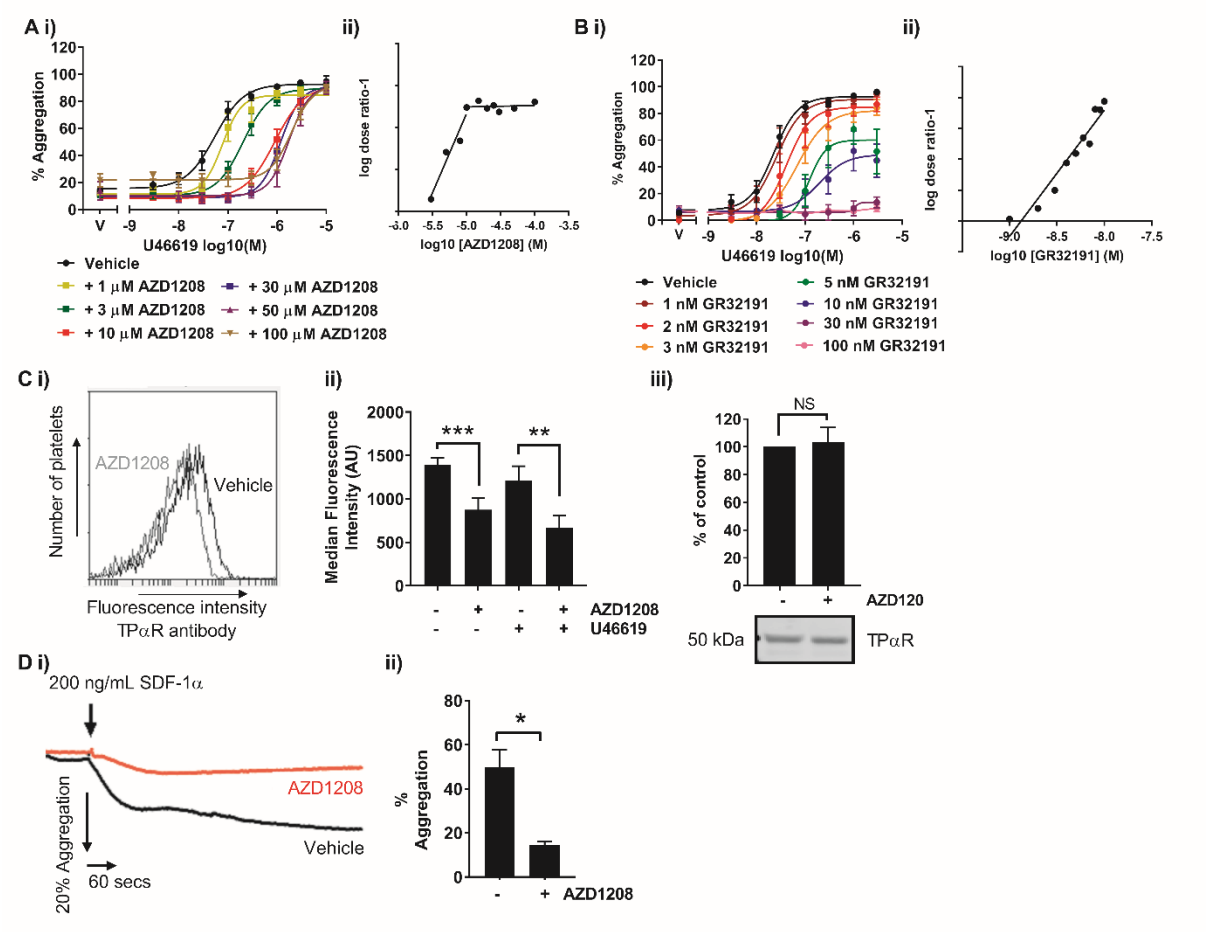
A i)
ii)
% Aggregation
U46619 log10(M)
log dose ratio-1
log10 [AZD1208] (M)
Vehicle
+ 1 μM AZD1208
+ 3 μM AZD1208
+ 10 μM AZD1208
+ 30 μM AZD1208
+ 50 μM AZD1208
+ 100 μM AZD1208
B i)
ii)
log10 [GR32191] (M)
Vehicle
1 nM GR32191
2 nM GR32191
3 nM GR32191
5 nM GR32191
10 nM GR32191
30 nM GR32191
100 nM GR32191
C i)
Number of platelets
AZD1208
Vehicle
Fluorescence intensity
TPαR antibody
ii)
Median Fluorescence Intensity (AU)
AZD1208
U46619
iii)
% of control
NS
AZD120
50 kDa
TPαR
D i)
200 ng/mL SDF-1α
AZD1208
Vehicle
20% Aggregation
60 secs
ii)
% Aggregation
AZD1208

Figure 6

ONLINE DATA SUPPLEMENT

Anti-platelet properties of Pim kinase inhibition is mediated through disruption of thromboxane A2 receptor signalling.

AJ Unsworth, AP Bye, T Sage, RS Gaspar, N Eaton, C Drew, A Stainer, N Kriek, PJ Volberding, JL Hutchinson, R Riley, S Jones, SJ Mundell, W Cui, H Falet, JM Gibbins

MATERIALS AND METHODS

Reagents

AZD1208, CX-6258, LGH447, SGI-1776 and SMI-4a were purchased from SelleckChem. U46619 was purchased from Enzo Life Sciences (Exeter, UK). Bovine thrombin and ADP were purchased from Sigma Aldrich (Poole, UK). Horm collagen was purchased from Nycomed, Austria, CRP-XL from Prof. R Farndale (University of Cambridge, UK). Primary anti- TxA_2R (P20), Pim-1 and actin (C11) antibodies were purchased from Santa Cruz Biotechnology (Calne, UK). Primary antibodies for Pim-1, Pim-2 and Pim-3 (cat. Log #9779), anti-Phospho–PKC substrate antibody (#2261), Caspase-3 (#9662), cleaved caspase 3 (#9661) and phospho-Ser19 Myosin light chain (#3671) antibodies were purchased from New England Biosciences (Cell Signalling Hitchin, UK), anti-phospho-Ser 4A4 antibody was purchased from Millipore (Watford, UK), anti-TP receptor (ab137607) and DOK6 (ab72730) antibodies were purchased from Abcam (Cambridge, UK). Fluorophore conjugated secondary antibodies, Fluo-4 calcium indicator dye and Alexa-488 conjugated phalloidin were purchased from Life Technologies (Paisley, UK). All other reagents were from previously described sources.

Mice

Global *Pim1*$^{-/-}$ mice were described previously [1,2]. Genotyping was confirmed by PCR of tail tissue DNA using primers: AAGCACGTGGAGAAGGACCG (WT forward), GACTGTGTCCTTGAGCAGCG (WT reverse; *Pim1*$^{+}$ 487bp), and CGTCCTGCAGTTCATTCAGG (Neo reverse; *Pim1*$^{-}$ ~360bp). Due to breeding strategy age and litter matched Pim-1$^{+/-}$ mice were used as controls. Pim-1$^{+/-}$ mice were found to show no difference in platelet function to C57BL/6 WT mice (data not shown). Mice used were C57BL/6 of both sexes, aged 7-10 weeks, and were treated according to the National Institutes of Health and Medical College of Wisconsin Institutional Animal Care and Use Committee guidelines and following procedures approved by the University of Reading Research Ethics Committee.

Platelet preparation

For mouse experiments, blood was collected by mouse retro-orbital plexus bleeding and was anticoagulated in acid-citrate-dextrose [3]. Platelet-rich plasma was obtained by centrifugation of the blood at 100 g for 8 min, followed by centrifugation of the supernatant and buffy coat at 100 g for 6 min. After washing twice in washing buffer (140 mM NaCl, 5 mM KCl, 12 mM trisodium citrate, 10 mM glucose, and 12.5 mM sucrose, pH 6.0), platelets were resuspended at 4 x 10^8 platelets/ml in resuspension buffer (140 mM NaCl, 3 mM KCl, 0.5 mM $MgCl_2$, 5 mM $NaHCO_3$, 10 mM glucose, 10 mM HEPES, pH 7.4) and were allowed to rest for 30 min before use.

For human experiments, blood was obtained from consenting aspirin-free healthy volunteers following procedures approved by the University of Reading Research Ethics Committee.

Blood was collected into 4% (w/v) sodium citrate and then mixed with acid citrate dextrose (29.9 mM trisodium citrate, 113.8 mM glucose and 2.9 mM citric acid [pH 6.4]) if washed platelets were prepared. Platelet rich plasma (PRP) was prepared by centrifugation at 100 g for 20 minutes at room temperature. ADP sensitive washed platelets were prepared from PRP (containing ACD) by centrifugation at 350 g for 20 minutes followed by resuspension in modified Tyrode's-HEPES buffer (134mM NaCl, 0.34mM Na_2HPO_4, 2.9mM KCl, 12mM $NaHCO_3$, 20mM N-2-hydroxyethylpiperazine-N-2-ethanesulfonic acid, 5mM glucose and 1mM $MgCl_2$, pH 7.3) and used immediately.

Thrombus formation on collagen under flow *in vitro*

Thrombus formation on and platelet interaction with immobilized type I collagen was performed as described previously [4] using the VenaFlux Platform and Vena8Fluor+ Biochips (Cellix) [5]. Channels were coated overnight at 4°C with collagen, then blocked with 1% BSA/PBS for 1 h and replaced with PBS. Mouse blood was collected by retro-orbital plexus bleeding and was anticoagulated in 25 mM PPACK. Human blood was collected into sodium citrate (4% w/v). Platelets in whole blood were incubated with 10 mM DiOC6 (Thermo Fischer Scientific) for 10 min. Perfusion was performed for either 4 min (mouse) or 12 minutes (human) at 37°C with an arterial shear rate of 1500 s^{-1}. For mouse, platelet adhesion to the collagen-coated chip was monitored with an Axioscope A.1 Inverted Microscope (Carl Zeiss) at 20x magnification through a Digital CCD Camera C10600-10B (Hamamatsu Photonics). Human thrombus formation was visualised using a 20 x magnification lens on a Nikon A1-R confocal microscope. Images were brightness corrected and converted to a binary mask with software provided auto-thresholds. Binary Mask Particles were then analysed to determine thrombus count and surface area.

$FeCl_3$ injury thrombosis model

Male C57BL/6 mice (8 – 10 weeks of age) were anesthetized through an intraperitoneal. injection of ketamine (100 mg/kg), metedor (20 mg/kg) and atropine (0.25 mg/kg) and injected with DIOC6 to fluorescently label platelets (0.28 µL of a 1mg/mL solution per body weight). AZD1208 (0.16 µL of a 100 mM solution per body weight) or vehicle control were injected immediately before isolation of mesenteric arteries. Vascular injury was induced by applying a 1 mm^2 Whatmann filter paper saturated with 10% $FeCl_3$ for 90 seconds and images recorded for at least 20 minutes. Images were acquired using a Hamamatsu digital camera C9300 (Hamamatsu Photonics UK Ltd) and Olympus BX61W1 microscope (Olympus Imaging Ltd, UK) and analysed using Slidebook5 (Intelligent Imaging Innovations, USA).

Tail bleeding

Bleeding time in Pim-$1^{-/-}$ and Pim-$1^{+/-}$ mice was determined by transecting 2 mm of distal mouse tail and immediately immersing the tail in 37°C isotonic saline [3]. A complete cessation of bleeding was defined as the bleeding time. Measurements exceeding 10 min were stopped by cauterization of the tail.

Tail bleeding experiments with Pim kinase inhibitors were performed on 20–35 g male mice, anesthetized with ketamine (100 mg/kg) and xylazine (10 mg/kg) injected intraperitoneally. AZD1208 (100 µM) or vehicle control (DMSO 0.1% v/v) was injected into the femoral vein 10 minutes prior to removal of the tip of the tail. The tail tip was then placed in sterile saline (37 ºC) and time to cessation of bleeding (secs) measured.

Platelet aggregation

Aggregation of human washed platelets was measured by optical aggregometry (Helena Biosciences, Gateshead, UK) as described previously [6]. Endpoint aggregation measurements were also taken using a plate based assay in which PRP or washed platelets at a concentration of $4x10^8$ cells/ml were loaded onto 96-well half-area plates (Greiner) and treated with inhibitors or vehicle for 10 mins at 37° C prior to addition of agonist. Plates were shaken at 1,200 rpm for 5 mins at 37° C using a plate shaker (Quantifoil Instruments) and absorption of 405 nm light measured using a NOVOstar plate reader (BMG Labtech).

Alpha granule secretion and fibrinogen binding by flow cytometry

Flow cytometry was used to examine alpha granule secretion and affinity up-regulation of the integrin $\alpha_{IIb}\beta_3$ by detecting levels of P-selectin exposure and fibrinogen binding respectively . Following inhibitor or vehicle treatment for 10 minutes and stimulation with U46619, platelets were incubated at room temperature for 20 minutes with PE/Cy5 anti-human CD62P (P-selectin) and fluorescein isothiocyanate-labelled (FITC) anti-fibrinogen antibody. Reactions were stopped and platelets fixed by addition of 0.2% (v/v) paraformaldehyde. Data for 5000 events were collected using a BD Accuri C6 flow cytometer and analysed using the CFlow Sampler software as described previously [4].

TxB_2 generation assay

PRP was stimulated with either 3 µg/mL Collagen or 100 µM Arachidonic acid, both in the presence and absence of 100 µM AZD1208 or indomethacin (10 µM) at 37 °C with shaking at 1200 rpm on a plate shaker. The reaction was stopped after 5 min by the addition of 50 µM indomethacin and 2 mM EDTA, and the cell debris removed by centrifugation. Samples were diluted 1/100 in assay buffer provided prior to testing. The TxB_2 assay was performed using an assay kit (Enzo Life Sciences (UK) Ltd, Exeter UK) according to the manufacturer's specification and the 96-well ELISA plate read on a FlexStation microplate reader (Molecular Devices). Data analysis was subsequently conducted using a standard curve constructed from a serial dilution of working standard samples to calculate TxB_2 production.

Mobilisation of intracellular calcium

PRP was loaded with Fura-2 AM (2 µM) for 1h at 30°C and then washed by centrifugation at 350 g for 20 mins and resuspended in Tyrode's-HEPES buffer containing 0.4 U/ml apyrase. Fura-2 loaded platelets were incubated with inhibitors or vehicle at 37°C prior to addition of agonists. Fluorescence measurements with excitation at 340 and 380 nm and emission at 510 nm were recorded over a period of 5 mins using a NOVOstar plate reader (BMG Labtech). $[Ca^{2+}]_i$ was estimated using the ratio of the 340 and 380 nm excited signals and the method of Grynkiewicz *et al* was utilised [7]. The maximum fluorescence ratio was measured following treatment with 50 µM digitonin and the minimum fluorescence ratio measured following treatment with 10 mM EGTA. Autofluorescence was also corrected for, using platelets which had not been loaded with Fura-2. $[Ca^{2+}]_i$ concentrations were calculated as described previously [8,9].

Immunoblotting and immunoprecipitation

Washed platelets (4×10^8 cells/mL) were lysed in an equal volume of NP40 buffer (300 mM NaCl, 20 mM Tris base, 2 mM EGTA, 2 mM EDTA, 1 mM PMSF, 10 µg/ml aprotinin, 10 µg/ml leupeptin, 0.7 µg/ml pepstatin A, 2 mM sodium orthovanadate, 2% NP-40, pH 7.3) for lysate

preparation for immunoprecipitation or lysed with 6 x Laemlli sample buffer for directanalysis by western blotting. For immunoprecipitation proteins of interest were isolated using 1 µg of appropriate antibodies as described previously [6]. Immunoblotting was performed using standard techniques as described previously [10].
Proteins were detected using fluorophore conjugated secondary antibodies and visualised using a Typhoon Fluorimager and Image Quant software (GE Healthcare). Band intensities were quantified and levels of the immunoprecipitated protein were used to normalize the phosphorylation data using Image Quant software.

Surface expression of TPαR by flow cytometry
Flow cytometry was used to determine surface expression levels of the TP receptor. Following inhibitor or vehicle treatment for 10 minutes and stimulation by U46619. Platelets were incubated at room temperature for 20 minutes with anti-human TP receptor (Abcam) that recognises the extracellular portion of the TP receptor and Alexa647 conjugated anti-rabbit secondary antibody. Anti-DOK6 antibody (Abcam) was used as a negative control. Reactions were stopped by dilution in HEPES- buffered saline and analysed immediately. Data for 10,000 events were acquired using a BD Accuri C6 flow cytometer and analysed using the CFlow Sampler software.

Statistics
All experiments were performed at least in triplicate. Statistical analyses of the data were carried out using GraphPad prism software. When comparing two sets of data, an unpaired, 2-tailed Student's t test (simple) statistical analysis was used. If more than two means were present, significance was determined by one-way or two-way ANOVA followed by Bonferroni correction (multiple) or the Kaplan-Meier analysis (time-to-event). Where data was normalised, statistical analysis was performed prior to normalisation and also using the non-parametric Wilcoxon signed-rank test. $P \leq 0.05$ was considered statistically significant. Unless stated otherwise, values were expressed as mean ±SEM.

Study approval
For experiments using human blood, procedures and experiments were approved by the University of Reading and Manchester Metropolitan University Research Ethics Committees. Mice used were treated according to the National Institutes of Health and Medical College of Wisconsin Institutional Animal Care and Use Committee guidelines and as following procedures approved by the University of Reading Research Ethics Committee.

SUPPLEMENTAL DATA

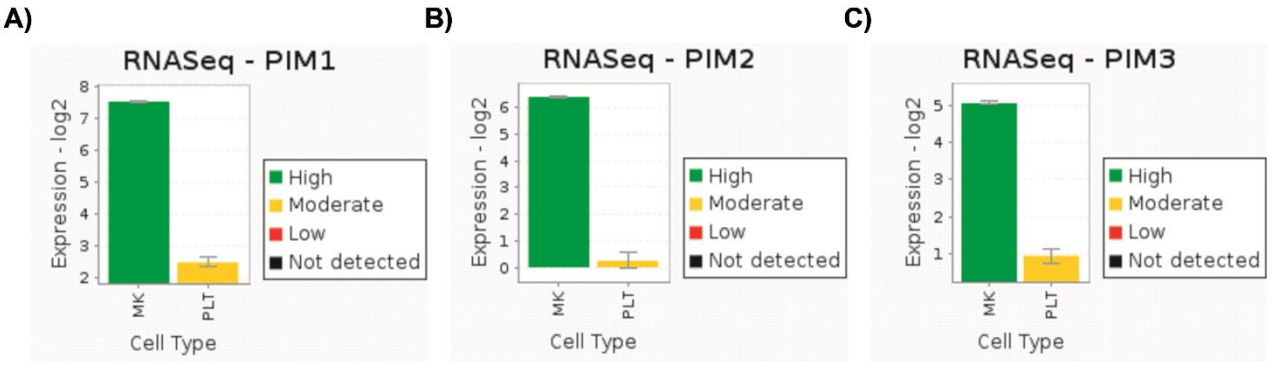

Supplemental Figure 1. Expression of Pim kinase in human megakaryocytes and platelets. RNA seq analysis of A) Pim-1, B) Pim-2 and C) Pim-3 mRNA-seq expression in megakaryocytes and platelets from 5 different data sets, taken from the HAEMGEN Tools portal Expressed! https://haemgen.haem.cam.ac.uk/expressed

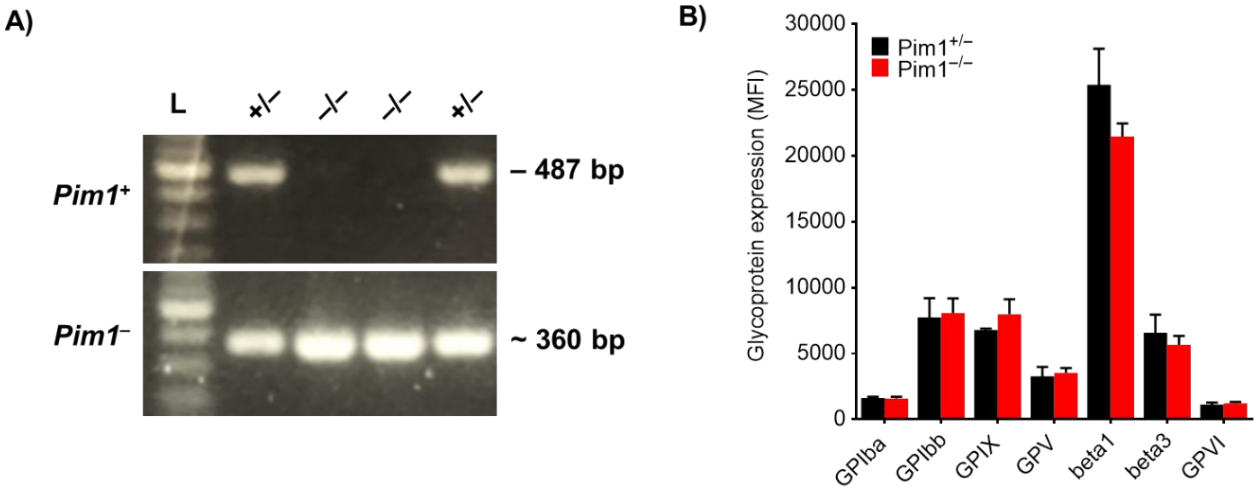

Supplemental Figure 2. Pim-1$^{-/-}$ deficient platelets have normal receptor expression levels. A) Global *Pim1*$^{-/-}$ mice genotyping was confirmed by PCR of tail tissue DNA using primers: AAGCACGTGGAGAAGGACCG (WT forward), GACTGTGTCCTTGAGCAGCG (WT reverse; *Pim1*$^{+}$ 487bp), and CGTCCTGCAGTTCATTCAGG (Neo reverse; *Pim1*$^{-}$ ~360bp). B) Expression levels of different platelet surface receptors, GPIba, GPIbb, GPIX, GPV, Beta1, Beta3 and GPVI were determined by flow cytometry in platelets from Pim-1$^{+/-}$ and Pim-1$^{-/-}$ mice. Results are mean ± S.E.M. for n≥3, * indicates $p<0.05$ in comparison to controls.

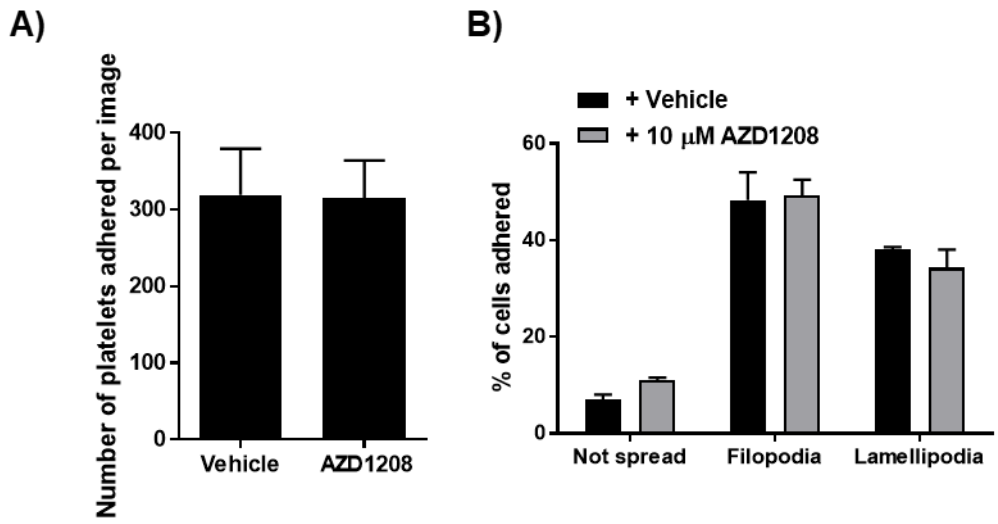

Supplemental Figure 3. Pim kinase inhibition does not alter adhesion to collagen. . Human washed platelets pretreated with 10 µM AZD1208 or vehicle control were exposed to collagen (100 µg/mL) coated coverslips and left to adhere and spread for 1 hour at room temperature. A) Adhesion, number of platelets adhered were counted in 5 randomly selected fields of view and expressed as the average number of cells per image. B) Spreading, platelets were classified into 3 different categories to determine the extent of their spreading (Adhered but not spread, Filopodia: platelets in the process of extending filopodia and Lamellipodia: platelets in the process of extending lamellipodia including those fully spread). Results expressed as relative frequency, as a percentage of the total number of platelets adhered. n≥3.

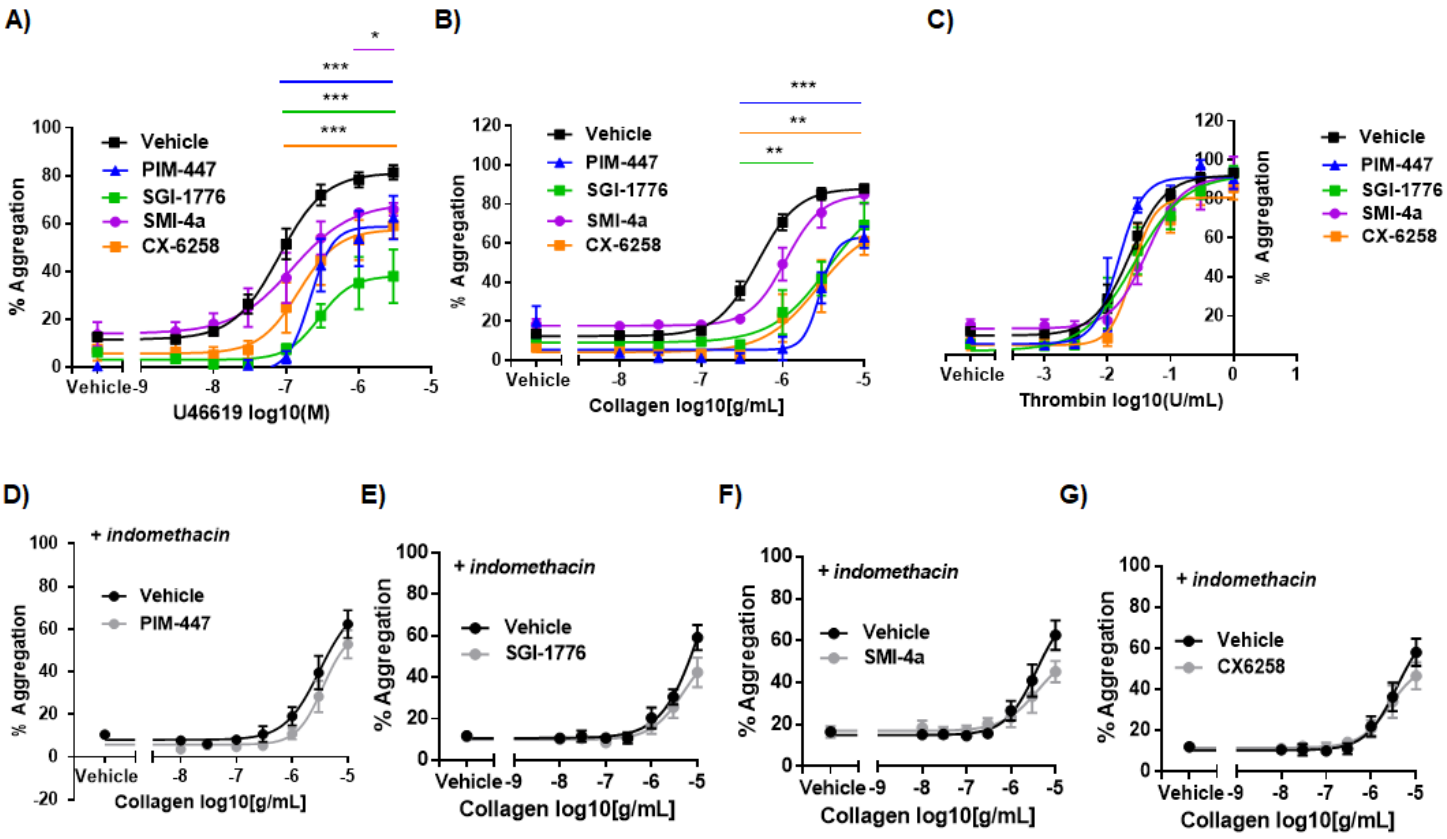

Supplemental Figure 4. Structurally distinct Pim kinase inhibitors attenuate platelet activation by the TP receptor. (A-C) Human washed platelets were pre-treated with different PIM kinase inhibitors PIM-447 (LGH-447) (10 µM) (blue) SGI-1776 (10 µM) (green), SMI-4a (30 µM) (purple), CX-6258 (10 µM) (orange) or vehicle control (black) prior to stimulation with i) U46619 (3 nM- 3µM), ii) collagen (0.01-10 µg/mL) or iii) Thrombin (0.01-1 U/mL). (D-G) Human washed platelets were treated with A) 10 µM PIM447 (LGH447), B) 10 µM SGI-1776, C) 30 µM SMI-4a or D) 10 µM CX6258 (grey) in the presence of indomethacin prior to stimulation y collagen (0.01-10 µg/mL) and aggregation was monitored after 5 minutes using an optical light transmission plate based aggregometry assay, quantified data shown. Results are mean + S.E.M. for n≥3, * indicates $p<0.05$ in comparison to controls.

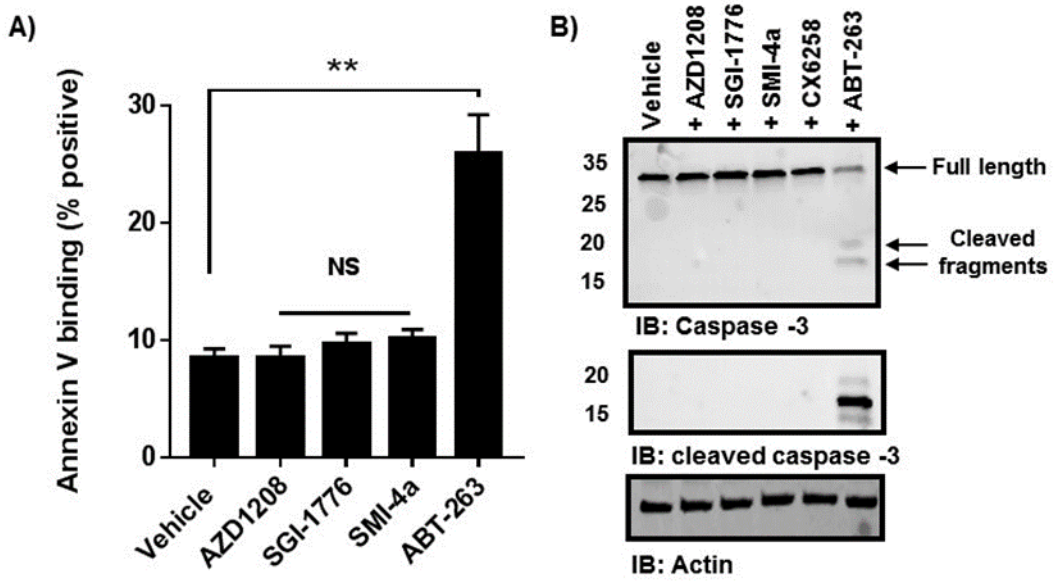

Supplemental Figure 5. AZD1208 does not cause apoptosis in platelets. Human washed platelets were treated for 2 hours with or without A) AZD1208 (10μM), SGI-1776 (10μM), SMI-4a (30μM), ABT-263 (10 μM) or vehicle control prior to analysis by flow cytometry for Annexin V binding which is a measure of phosphatidylserine exposure, a marker of apoptosis. Data are expressed as % positive events for Annexin V. B) Platelets were incubated with AZD1208 (10μM), SGI-1776 (10μM), SMI-4a (30μM) or CX6258 (10μM) for 2 hours and lysed in Laemmli sample buffer. Samples were then run on SDS PAGE gels, transferred to PVDF membrane before blotting for caspase-3 or cleaved caspase-3 (a marker of apoptosis). Actin was included as a loading control. ABT-263 (10 μM) a Bcl-2 inhibitor and known initiator of apoptosis in platelets was included as a positive control. Results are mean ± S.E.M. for n≥3, * indicates $p<0.05$ in comparison to vehicle controls.

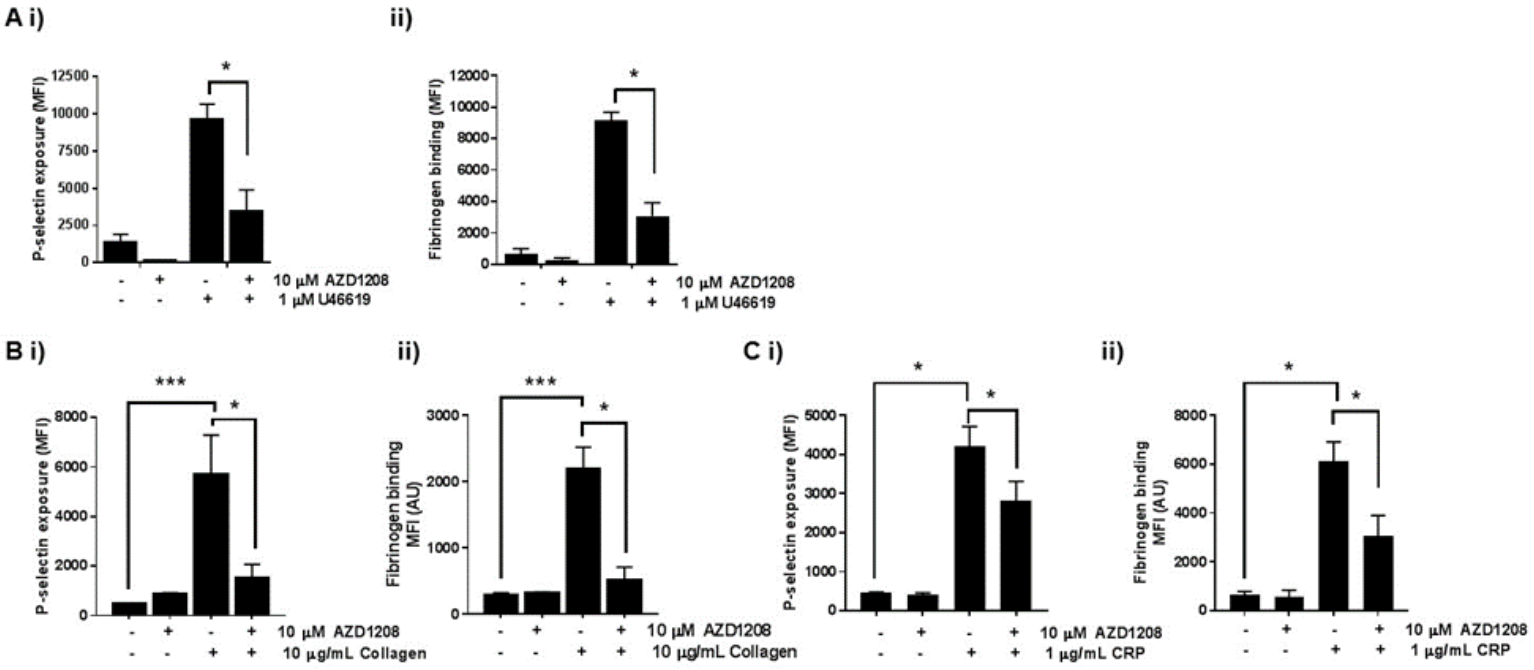

Supplemental Figure 6. AZD1208 attenuates alpha granule secretion and integrin αIIbβ3 activation. Resting and stimulated human washed platelets were treated with 10 µM AZD1208 prior to stimulation with A) U46619 (1 µM), B) Collagen (10 µg/mL) or C) CRP (1 µg/mL) and i) Alpha granule secretion determined by monitoring P-selectin exposure and ii) Integrin activation measured as fibrinogen binding. Results are mean + S.E.M. for n≥3, * indicates $p<0.05$ in comparison to vehicle controls.